University of South Bohemia in České Budějovice

Faculty of Science

Recombinant production and characterization of protease domain from TBEV nonstructural protein NS3

Master thesis

Bc. Kateřina Vejvodová

Supervisor: RNDr. Zdeněk Franta, Ph.D.

Co-supervisor: Paulina Duhita Anindita DVM, Ph.D.

České Budějovice 2021

Vejvodová K., 2021: Recombinant production and characterization of protease domain from TBEV nonstructural protein NS3, Master thesis, in English – 74 p., Faculty of Science, University of South Bohemia, České Budějovice, Czech Republic.

Annotation

The aim of this thesis was to produce and characterize recombinant protease domain of TBEV nonstructural protein 3 (NS3). The NS3 protein of TBEV is essential in viral replication and plays an indispensable role in cleaving viral polyprotein into structural and nonstructural viral proteins, thus making it an attractive target for antiviral treatment. This thesis summarized the cloning of TBEV NS3 protease, production and purification of recombinant enzyme, biochemical and kinetic characterazion of the protease domain from TBEV NS3.

Sworn declaration:

I hereby declare that I have worked on my master's thesis independently and used only the sources listed in the bibliography.

České Budějovice, 30.4.2021

…….

Bc. Kateřina Vejvodová

Acknowledgements:

First and foremost, I would like to extend my deepest gratitude to my supervisor RNDr. Zdeněk Franta, Ph.D and co-supervisor Paulina Duhita Anindita DVM, Ph.D. for their guidance, valuable advices, support and assistance. Thank you so much for taking the time for sharing your knowledge with me.

My acknowledgements also intend to whole collective in the laboratory Makrokomplex. Namely Zuzana Světelová, who was always kind to answer my questions and help. I could not have better colleagues than you.

Lastly, I am indebted to my family for their love, understanding and support.

Table of contents

List of abbreviations

aa – amino acid

AEC – anion exchange chromatography

AMP – ampicilin

AMP-PNP – β,γ-Imidoadenosine 5′-triphosphate lithium salt hydrate

Ala – alanine

APS – ammonium persulfate

Arg – arginine; R – arginine

Asp – asparatic acid

Asn – asparagine

ATP – Adenosine Triphospate

ATPase – adenosine triphosphatase

bp – base pair

BPTI – bovine pancreatic trypsin inhibitor

C – capsid

CAM - chloramphenicol

CV – column volume

ddH_2O – double-distilled water

dNTP – deoxynucleotide triphosphate

ds RNA – double-stranded RNA

DENV – Dengue virus

E – envelope

ER – endoplasmatic reticulum

EDTA – ethylenediaminetetraacetic acid

Em – emission

EU – The European Union

EEA – The European Economic Area

Ex – excitation

GA – Golgi apparat

Glu – glutamic acid

Gln – glutamine

Gly – glycine

His – histidine

HIV – human immunodeficiency virus

ID – identity document

IMAC – immobilized metal affinity chromatography

IPTG – isopropyl β-D-1- thiogalactopyranoside

JEV – Japanese encephalitis virus

kb – kilobase

kDa – kilodalton

Km – the Michaelis-Menten constant

Kcat – the catalytic rate constants

LB – lysogeny broth

LBP – lamin-binding protein

Leu – leucine

Lys – lysine; K – lysine

M – membrane

mRNA – messenger RNA

min – minute

MTase – methyl transferase

NC – nucleocapsid

NMR – nuclear magnetic resonance spectroscopy of proteins

Nle – norleucine

NSP – nonstructural protein

NS1 – nonstructural protein 1

NS2A – nonstructural protein 2A

NS2B – nonstructural protein 2B

NS2Bcof – nonstructural protein 2B cofactor

$NS2B_{47}$ – residues 49-96 of NS2B protein

NS3 – nonstructural protein 3

NS3pro – nonstructural protein 3 protease domain

NS3hel – nonstructural protein 3 helicase domain

NS4A – nonstructural protein 4A

NS4B – nonstructural protein 4B

NS5 – nonstructural protein 5

NTP – nucleoside triphosphates

OD_{600} – optical density measured at 600 nm

ON – overnight

PAGE – polyacrylamide gel electrophoresis

PCR – polymerase chain reaction

PDB – protein data bank

prM – precursor membrane

PVDF membrane – Polyvinylidene fluoride

RdRP – RNA-dependent RNA polymerase

RC – replication complex

RNA – ribonucleotide acid

RTPase – RNA triphosphatase

SDS – sodium dodecyl sulfate

SEC – size exclusion chromatography

Ser – serine

S.O.C. medium – super optimal broth with catabolite repression

SDS-PAGE – sodium dodecyl sulphate-polyacrylamide gel electrophoresis

SP – structural protein

ssDNA – single-stranded DNA

ssRNA – single-stranded RNA

SF – super family

TAE –tris-acetate-EDTA (Ethylenediaminetetraacetic acid)

TBEV – Tick-borne encephalitis virus

TBEV-Eu – Tick-borne encephalitis virus – European sub-type

TBEV-Sib – Tick-borne encephalitis virus –Siberian sub-type

TBEV-FE – Tick-borne encephalitis virus –Far-Eastern sub-type

TBS – tris-buffered saline

TEMED – tetramethylethylenediamine

Thr – threonine

UV– ultraviolet

WNV – West Nile virus

Xaa – any amino acid

YFV –Yellow Fever virus

ZIKV – Zika virus

ZRR-AMC- Z-Arginine-Arginine-7-amido-4-methylcoumarin hydrochloride

Abstract

Tick-borne encephalitis virus (TBEV) is a causative agent of tick-borne encephalitis (TBE) one of the most important diseases representing a growing health problem in Europe. Most TBE cases are asymptomatic; however, the disease can lead to an irreversible neurological complications or death. Although a TBEV specific vaccine is currently available to prevent TBEV infection and transmission in the endemic areas, the incidence of infections is constantly rising. Moreover, up to now, there is no antiviral treatment to treat TBE patients. Nonstructural (NS) proteins of TBEV are involved in viral replication thus representing feasible targets for antiviral treatment. Among the NS proteins, NS3 protease (NS3pro) plays an indispensable role in processing of viral polyprotein into structural and nonstructural viral proteins, making it an attractive target for antiviral drug design. Therefore, a deeper understanding of NS3pro activity together with atomic resolution structure is required to foster the development of antiviral treatment against TBEV.

1 Introduction

1.1 Tick-borne encephalitis virus (TBEV)

TBEV is a member of the genus *Flavivirus*, family *Flaviviridae*. The name is sought after yellow fever virus (YFV) derived from febris flava; the word flavus means 'yellow' in Latin [1]. Many flaviviruses are arthropod-borne meaning that they are transmitted into a vertebrate host by an arthropod vector (mosquito or tick). TBEV, DENV, WNV, ZIKV, JEV are well known flaviviruses causing severe diseases in human [2, 3].

To date, there is no antiviral treatment against flavivirus infection although safe and relatively effective vaccines are available for some viruses such as TBEV, YFV and JEV [4, 5]. Therefore, the general countermeasures to combat the spread of flaviviruses are limited to preventing contact between the arthropod vectors and humans using public health approaches [6, 7].

1.1.1 Transmission of TBEV

TBEV is mainly transmitted by the bite of infected tick, or by a less common way via consumption of raw milk or non pasterized milk products from infected ruminants. In Europe, *Ixodes ricinus* and *Ixodes scapularis* (class *Arachnida*, subclass *Acari*) serve as vectors of TBEV [3,7].

Transmission of TBEV in ticks (Figure 1) occures in several ways. TBEV is transmitted transstadially among different developmental stages in tick's life cycle - larva, nymph and adult tick. TBEV can also be trasmitted horizontally, between infected and uninfected developmental stages, which co-feed on the same vertebrate host. In the case of transovarial transmission, TBEV is transmitted from an infected adult tick to the eggs [8, 9] There is no known direct human-to-human or animal-to-human transmission of TBEV and the horizontal trasmissoin is thought to be key for maintaining the circulation of TBEV in animal host [10, 11].

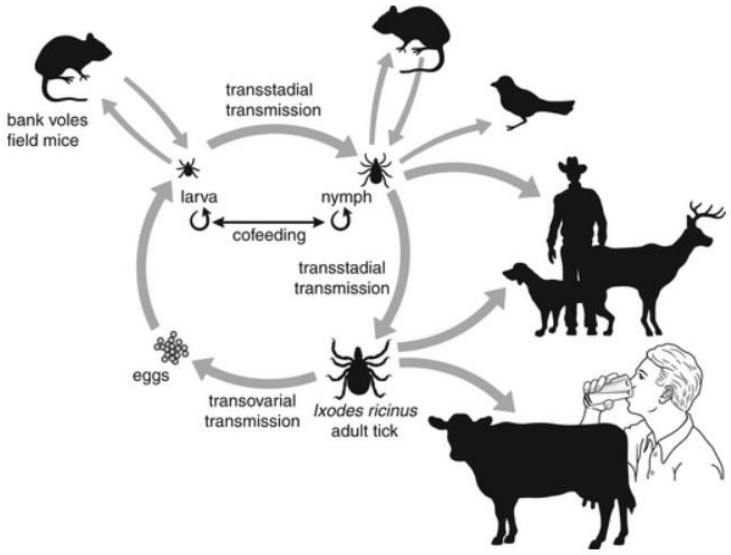

Figure 1**: Transmission of TBEV.** Adapted from [1].

1.1.2 Pathogenesis of TBEV infection

Most TBEV infections are asymptomatic; however, it can develop into neurological manifestations, such as meningitis, encephalitis or meningoencephalitis [3, 4]. The mortality and morbidity of TBE depends on the viral subtype: European (TBEV-Eu), Siberian (TBEV-Sib) and the Far-Eastern (TBEV-FE). The European subtype is associated with neurological consequences in up to 10% of patients and 0,5-2% mortality rate. In the case of the Siberian subtype, patients are prone to develop prolonged infections with 2-3% mortality rate. The Far-Eastern subtype is associated with hight rates of neurological consequences, with 40% mortality rate [12, 13]. Infection by Hypr strain from Europan subtypes has a typical two-phase character. The first phase is a primary viremia occuring after 1-2 weeks post-infection [14]. The virus replicates in the subcutaneous tissue and regional nodes. Subsequently, it is spread by blood and lymph to other lymphatic tissues. This phase manifests similarly to influenza symptoms (e. g. increased temperature, fatigue, headaches and muscle pain). The patient's condition usually improves after a few days and the healing may occur. If not, the disease will progress into the second phase which includes secondary viremia and finally significant health deterioration. In this phase, the virus enters the cerebrospinal fluid and meninges resulting in meningitis, meningoencephalitis or encephalomyelitis. The symptoms are high fever, headaches, vomiting, sleep disorders, cranial nerve disorders and limb paresis. Moreover, bleeding in the central nervous system as well as necrosis and degenerative changes of ganglion cells may occur [3, 15, 16].

Following the annual epidemiological report from ECDC for 2017 (Figure 2), 3 079 cases of tick-borne encephalitis were reported in EU/EEA countries, 2 550 (83%) of which were confirmed. The age and gender distribution shows a predominance of cases in 45-64 year olds and in males. TBE shows a seasonal pattern and in 2017, 78% of cases occurred from May-November, while 42% of cases occurred from June-August.

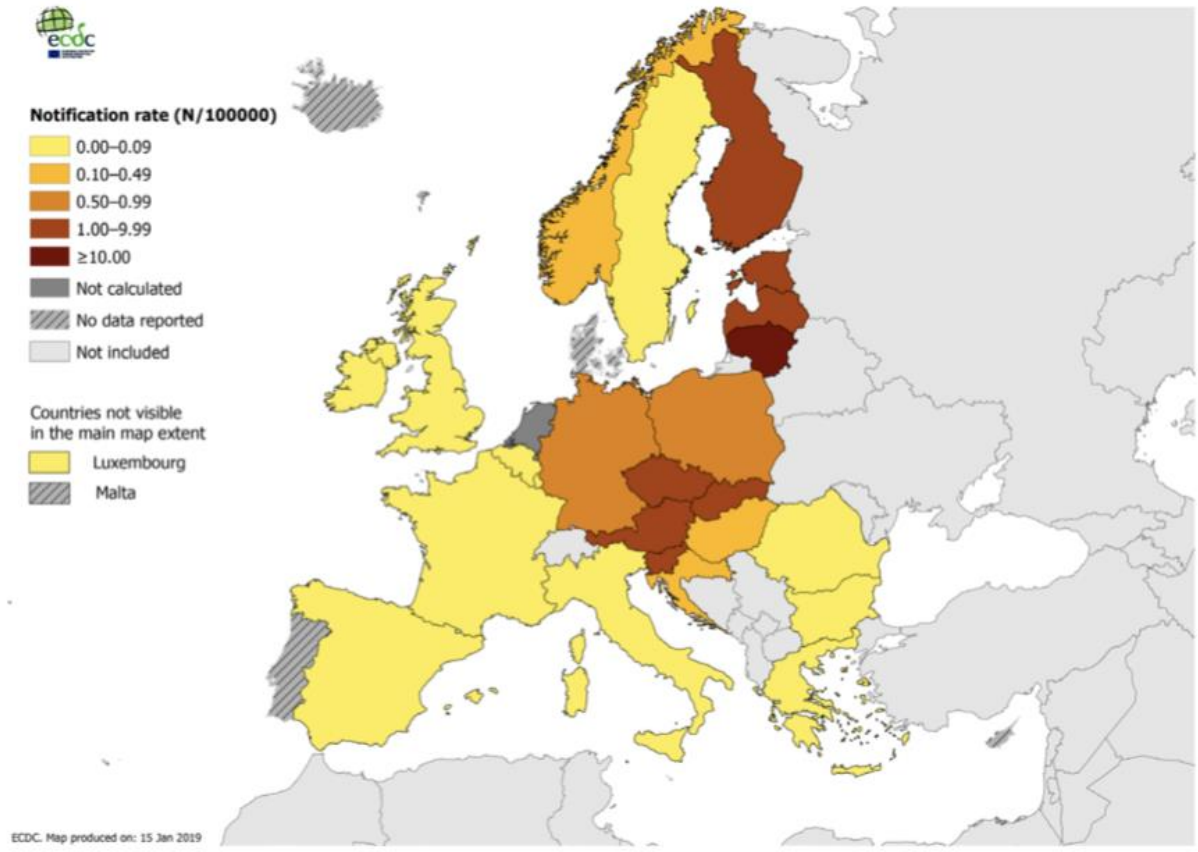

Figure 2**: Distribution of confirmed TBE case notification rate per 100,000 population by country in European Union/European Economic Area in 2017.** Adapted from [2].

1.2 Structure, genome and life cycle of TBEV

1.2.1 Structure of TBEV

TBEV has a 11 kb long, positive single-stranded RNA genome that encodes a single polyprotein [17]. A mature TBEV particle has a diameter of 50-60 nm, similar to other flaviviruses. One single polyprotein is co- and post-transcriptionally modified into three structural proteins (capsid, envelop and premembrane) and seven nonstructural proteins (NS1, NS2A, NS2B NS3, NS4, and NS5) [17, 18]. The virion consists of a nucleocapsid (NC) surrounded by a host-derived lipid membrane in which the viral envelope (E) and

membrane (M) proteins are embedded [19]. The nucleocapsid is composed of multiple copies of capsid protein (C) and a single copy of the (+) ssRNA genome [18,20] (Figure 3).

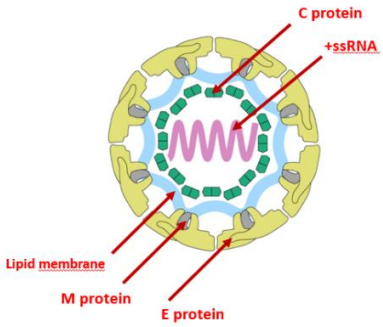

Figure 3: **Structure of TBEV virion**. Viral genome (lilac) is encapsulated by multiple copies of the C protein (green). The nucleocapsid is surrounded by a lipid membrane (light blue), in which E and M proteins (yellow and grey, respectively) are embedded. Adapted from [3].

The E and M proteins are highly organized and their arrangement determines the surface representation of the virion (Figure 4). These proteins assemble E-M-M-E heterodimers forming an icosahedral asymmetric unit of TBEV virion associated with the lipid envelope through their transmembrane domains [20-22].

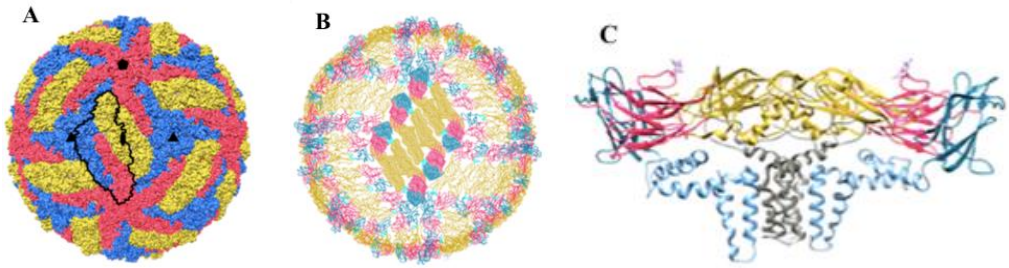

Figure 4: **Surface structure of the TBEV virion**. (A): The icosahedral asymmetric unit is outlined in black. E proteins are displayed in yellow, blue and red. (B): The three heterodimers of the E-M-M-E protein are shown, three E domains (red, blue and yellow) are visible on the surface, the turquoise color indicates a fusion loop. M proteins are not shown in this figure. (C): shows a heterodimer of proteins E and M (M proteins are shown in gray). Adapted from [3].

1.2.2 Life cycle of TBEV in mammalian cells

The life cycle of TBEV comprises several steps with a partial involvement of the host cell proteosynthetic apparatus (Figure 5). Firstly, TBEV virion interacts with host cell surface receptor (e. g. lamin-binding protein and αVβ3 integrin of mammalian cells [23]) and enters the cell via endocytosis pathway [24]. Following the entry step, the virion is enveloped by the cellular lipid layer and passed through cell compartments containing

different pH values. The low pH in the late endosome triggers the fusion of viral and endosomal membranes, leading to viral genome release from the virion [17, 24]. The viral genome is translated into a single chain polyprotein by the ribosomes of the rough endoplasmic reticulum. TBEV replicates its genome in specialized compartment called replication complex (RC), which is formed within the membrane of ER by assistance of viral nonstructural proteins and host factors. Newly synthesized viral genome is encapsidated by C protein. Nucleocapsid is formed and newly assembled virus particles containing E and prM proteins bud into the ER lumen [17, 18, 25]. Virions are trasported through the Golgi network undergoing maturation in the acidic environment of trans-GA due to conformational change of prM upon furin cleavage. Finally, matured virions as well as partially matured ones, bud out of the infected cell by membrane fusion which depends on the ratio of lipid membrane and cholesterol [26, 27]. These particles can start a new infection cycle however the particles, which are not matured are unable to bud out of the host cell and are non-infectious [18,28].

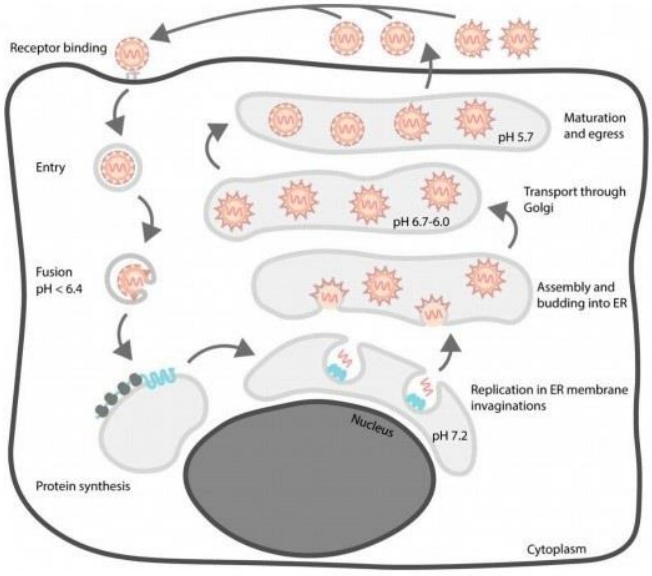

Figure 5: **An overview of the TBEV life cycle in mammalian cells**. Adapted from [3].

1.2.3 Replication complex (RC)

RC is formed inside membranous vesicle packets of ER membrane of infected cells (Figure 6). All NSs together with various host factors are required for efficient viral genome replication [1, 29]. In the RC, viral RNA-dependent RNA polymerase of NS5 synthesize the complementary negative strand (-) ssRNA, which then binds to the positive strand (+) ssRNA template resulting in a double-stranded dsRNA intermediate. After the unwinding of dsRNA intermediate by the helicase domain of NS3, nascent (+) ssRNA are

synthesized from the (-) ssRNA template. Newly synthesized (+) ssRNA binds to the (-) ssRNA and is released as the new dsRNA product, which serve as a template to generate more copies of (+) ssRNA. The pre-existing (+) ssRNA (genomic RNA) is then 5'-capped and methylated by the MTase domain of NS5 [30, 31]. This genomic RNA is subsequently captured by C proteins [32].

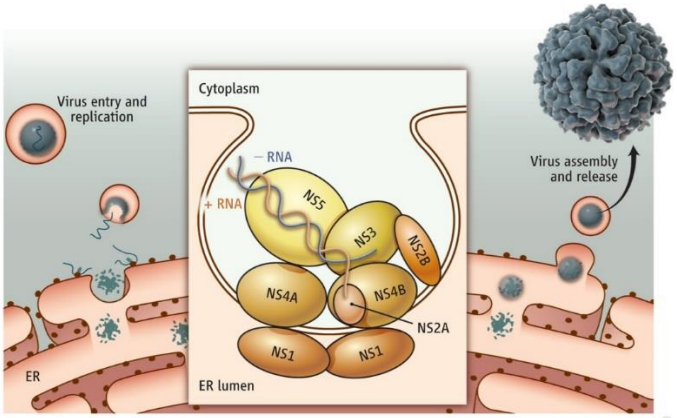

Figure 6: **Hypothetical scheme of TBEV replication**. Schematic depiction of the membrane bound flavivirus RC inserted in a protective vesicle. Adapted from [4].

1.2.4 Polyprotein processing

The viral genome (~ 11 000 bp) contains one open reading frame which is translated into a single polyprotein (~ 3,400 amino acids, aa) [18]. This polyprotein is subsequently cleaved by viral and host enzymes into individual functional proteins – structural proteins C, prM, and E and nonstructural proteins NS1, NS2A, NS2B, NS3, NS4A, NS4B, NS5 [33, 34].

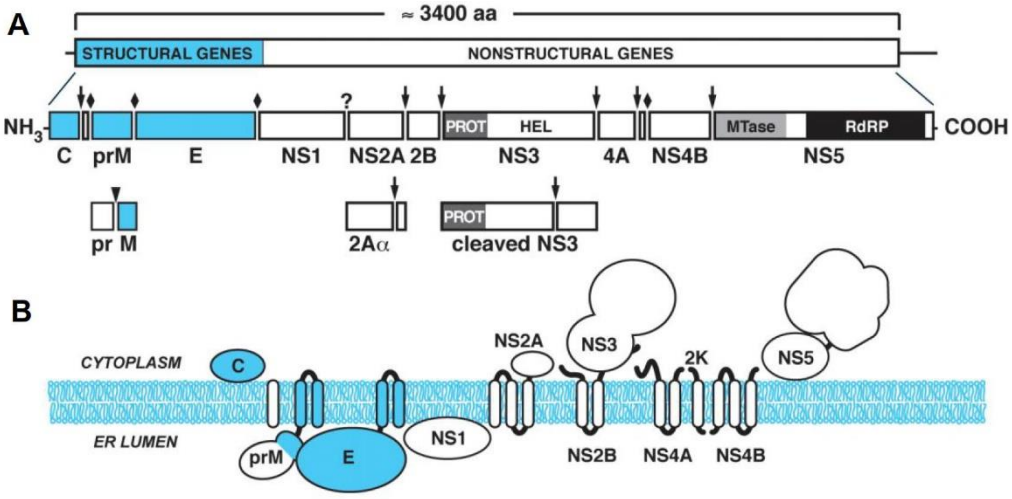

Figure 7: **TBEV genome structure and expression**· (A): Polyprotein processing and cleavage products. Structural proteins are colored blue, NS proteins are shown in white color. Cleavage sites for host signalase ♦,

the viral serine protease (↓), furin (▼), or unknown proteases (?) are indicated. (B): The proposed topology of the flavivirus polyprotein cleavage products with respect to the ER membrane is shown. The proteins are approximately to scale (areas are proportional to the number of amino acids) and arranged in order (left to right) of their appearance in the polyprotein. Structural genes are blue, NSP are shaded in grey. Adapted from [5].

The first translated NSP NS1 is a multi functional protein that exists in two forms. A dimer of NS1 is essential for virus replication [35], while NS1 hexamer is co-secreted with TBEV particles and has an immunomodulatory activity - it modulates the complement system in the mammalian hosts cells [35,36]. NSPs NS2A and NS2B are integral membrane proteins with a role in virus assembly [37]. NS2B serves also as a cofactor for the NS3 protease [37, 38]. NS2A is a non enzymatic NSP which is involved in immunomodulation and replication [39]. The NS3 N- terminal domain has a protease activity, the NS3 C- terminal NTPase dependent RNA helicase is essentiaal for virus replication and genome synthesis [28, 33, 40]. The integral membrane NS4A regulates an ATPase activity of NS3 helicase [40]. NS4A and NS4B are separated by a signal sequence of the 2k peptide [41, 42]. The 2k peptide is cleaved by the host signal peptidase and the NS4B remains integraded in the ER membrane and modulates host immune response [43] and it also participates in RC formation [41]. The NS5 contains two domains, the RNA-dependent RNA polymerase (RdRp) is required for virus genome replication, while the NS5 methyltransferase domain (MTase) caps the syntesized RNA [32, 44].

1.3 NS3 protein

NS3 protein is a multifunctional protein associated with ER membrane through an interaction with its NS2B cofactor. Among flaviviral proteins, NS3 is the second largest protein consisting of 621 aa with molecular weight of 69 kDa. Two domains of NS3 (N terminal protease domain and C-terminal helicase domain) are connected by a short flexible linker [45, 46] (Figure 8).

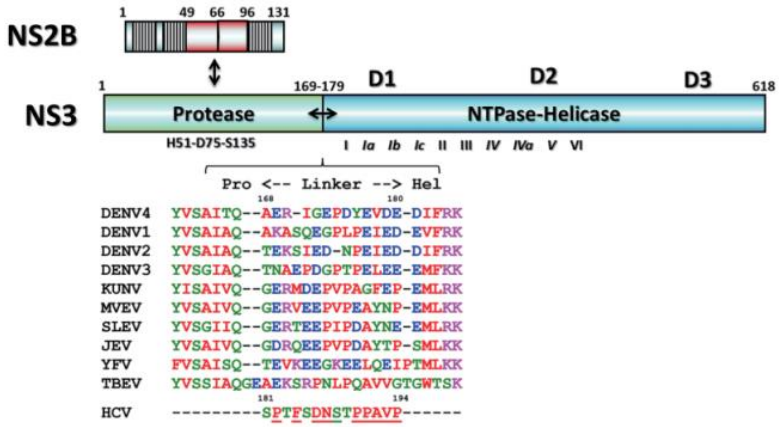

Figure 8: **Schematic representation of the flaviviral NS3 protein**. NS2Bcof is represented in the red region of NS2B. NS3 consists of the N terminal domain – protease, shown in green. The C terminal domain – NS3 helicase is in blue. Two segments of NS3 are connected with a linker. Adapted from [6].

1.3.1 NS3 helicase

The helicase domain of NS3 protein (NS3hel) belongs to the helicase superfamily 2 (SF2) [47]. It has three functional activities: RNA 5'-triphosphatase, nucleoside 5'- triphosphatase, and helicase carried by three subdomains. Eight conserved motifs, which are essential for ATP hydrolysis, RNA binding, and communication between these active sites are located within subdomain 1 and 2 [40, 47], while subdomain 3 assists the ssRNA binding (Figure 9).

Both NS3NTPase and RNA 5´triphosphatase share the same active site for ATP binding and hydrolysis [48]. While the RNA 5´triphosphatase activity is essential first step for viral RNA capping [49], NS3hel use the energy from ATP hydrolysis to unwind dsRNA thus helping the RdRp during the genome synthesis [50].

Figure 9: **Crystal structure of TBEV NS3hel**. (PDB ID: 7AY4), Anindita et al. manuscript in preparation.

1.3.2 NS3 protease

The N-terminal domain of NS3 has a protease activity in cooperation with the central region of NS2B, namely the NS2B-NS3 protease [32, 40]. This viral protease cleaves capsid protein and junctions between NS2A/NS2B, NS2B/NS3, NS3/NS4A and NS4B/NS5 [45, 49]. The NS2B (molecular weight: 16,6 kDa, 146 aa) is a membrane associated protein consisting of three domains: two transmembrane domains at the N- and C- terminal part and one central domain in which the cofactor activity toward NS3pro lies (NS2Bcof) (Figure 8) [37,51]. NS2B is necessary for proper folding of NS3pro. In the absence of NS2B cofactor, NS3pro is expressed as an insoluble protein [52]. It is also able to regulate NS3pro activity by stabilizing the correct protein fold of the core structure and also by directly participating in substrate cleavage [53].

Flavivirus NS2B-NS3 protease is a chymotrypsin like serine protease, which activity is determined by the conserved catalytic triad (His51, Asp75, Ser135) [54]. The protease recognizes and prefers a substrate, which has positively charged residue (Arg and Lys) at the P1 and P2 positions and a short side chain aa (Gly, Ser, or Ala) at P1' [54,55].

The protease activity is dependent on association with a hydrophilic region of 40 amino acids of the NS2B protein, which acts as a cofactor and actively participates in the formation of the S2 and S3 pockets in the protease active site [56]. Both viral and host proteases are required for viral polyprotein processing, which is essential for viral replication and virion assembly [57].

The active site of the flavivirus NS2B–NS3 protease is negatively charged and relatively flat, making it hard to design potent inhibitors by structure-based design (Figure 10). The preferred peptide substrate contains several positively charged amino acids in the non-prime side of the active site [56-58].

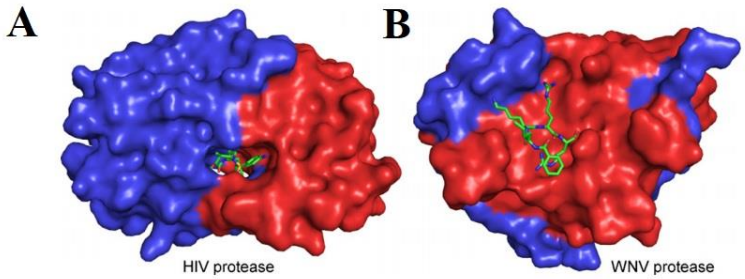

Figure 10: **Comparison of the HIV and WNV protease active sites.** A): The structures of the HIV protease dimer bound to Amprenavir® (PDB ID: 33EKV). (B): The structures of the WNV bound to a peptide inhibitor (PDB ID: 2FP7). Adapted from [7].

Currently, there is no available crystal structure of TBEV NS2B-NS3 protease although the crystal structure of other flaviviruses have been solved for WNV and DENV NS2B-NS3 as shown Figure 11 [62].

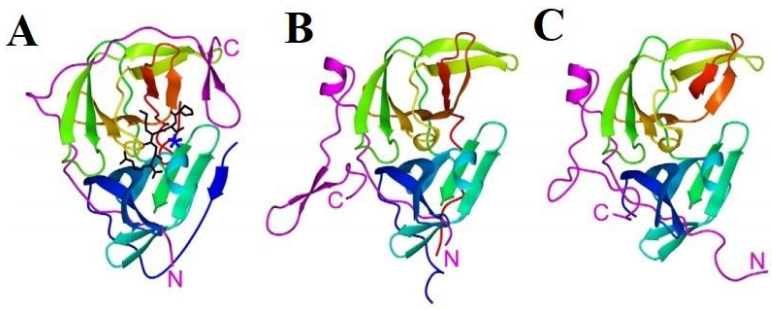

Figure 11: **Crystal structures of the West Nile and dengue NS2B-NS3 proteases**. (A): WNV NS2B-NS3pro in the presence of the inhibitor BPTI (PDB ID: 2IJO). The substrate binding site is indicated by the BPTI segment Pro13-Arg17 shown in black. The location of the active-site histidine is labeled with a blue star. (B): WNV NS2B-NS3pro in the absence of inhibitors. (C): Dengue virus NS2B-NS3pro in the absence of inhibitors (PDB ID: 2FOM).NS2B is shown in magenta, with the N- and C-termini labeled. The polypeptide chain of NS3 is shown in rainbow colors ranging from blue (N-terminus) to red (C-terminus). Adapted from [8].

WNV and DENV proteases have high sequence conservation (41% amino-acid identity within the protease region of NS3). NS2B is the most divergent between the two viruses (only 19% identity), particularly within the β hairpin (about 10% identity). Despite the high sequence conservation, WNV and DENV proteases have different sequence preferences in their cleavage sites [59, 60]. Peptide profiling for DENV-2 protease showed that it had a strong preference for basic amino acid residues (Arg/Lys) at the P1 positions, whereas the preferences for the P2– 4 sites were in the order of Arg > Thr > Gln/Asn/Lys for P2, Lys > Arg > Asn for P3, and Nle > Leu > Lys > Xaa for P4 [64]. This is different from WNV protease where the preferred P2 residue is K > R (Lys > Arg) [61, 62].

Author Li, et al, (2017) published that the mutations of the NS3 catalytic residues and the adjacent residues (V52, Y150, and G151) result in complete or almost complete loss of protease activity in DENV (Figure 12). Furthermore, a significant reduction in the protease activity is caused by a mutations of other adjacent residues of NS3 such as F130, G133 and N152 [49, 63], whereas mutations of (V154, V155, I139, I140, and G144) caused only moderate decrease in the protease activity [64]. Mutation of conserved residues in NS2B can have dramatic effects on autoproteolytic cleavage at the NS2B-NS3 junction and enzymatic activities [21, 65]. The NS2B mutation indicated that two regions are critical for protease function - region 1 and region 2. Region 1 is located between residues D58 and

W61, mutations of region 1 significantly decreased the protease activity. Region 1 is more conserved than those in region 2 of NS2B, suggesting that region 1 is critical for NS2B–NS3 recognition. Region 2 is located within the hairpin structure of NS2B (involving NS2B residues from L74 to I86) and is important for substrate specificity. Mutation of region 2 also reduced protease activity [66, 67].

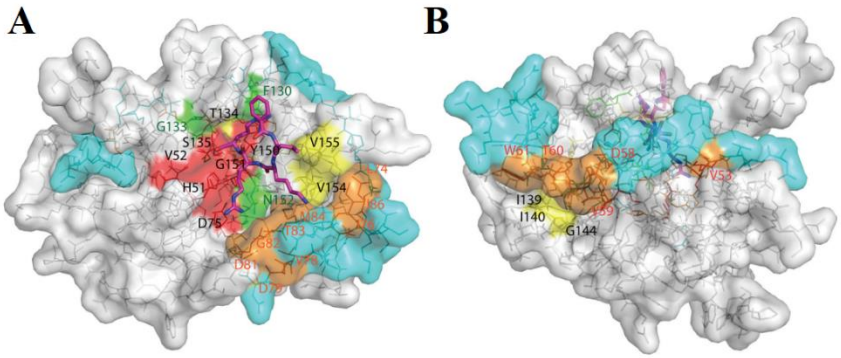

Figure 12: **Surface representation of mutagenesis results of the DENV3 NS2B-NS3 (PDB ID: 3U1I).** (A): View from active site. (B) View from behind the active site. The gray color of surface indicated NS3 and cyan indicated NS2B. The red color shown NS3 residues with mutations that led to completely or almost completely abolished the protease activity, the NS3 residues with mutations that significantly reduced protease activity are shown in green. The residues of NS3 that moderately affect the protease activity are in yellow. The orange color indicated the NS2B residues that are essential for the protease activity. Adapted form [9].

1.3.3 NS2B-NS3 protease as an antiviral target

Having the essential role in viral polyprotein processing and the inhibition of its activity interferes with viral replication, NS2B-NS3pro can serve as a good target for antiviral design. [52, 68]. There are two possible strategies to inhibit NS2B-NS3pro protease activity: (1) by blocking interactions with its substrate or (2) by blocking the essential association between NS3pro and its cofactor NS2B (Figure 13) [69, 70]. Most attention has been focused on the development of inhibitors that compete for the substrate-binding cleft. The preference of the substrate binding cleft of flaviviral proteases for ligands with basic residues at P1 and P2 might be exploited to provide inhibitors with specificity for NS2B-NS3pro. The second strategy of blocking the association of NS2B is novel and remains to be rigorously tested [70-72].

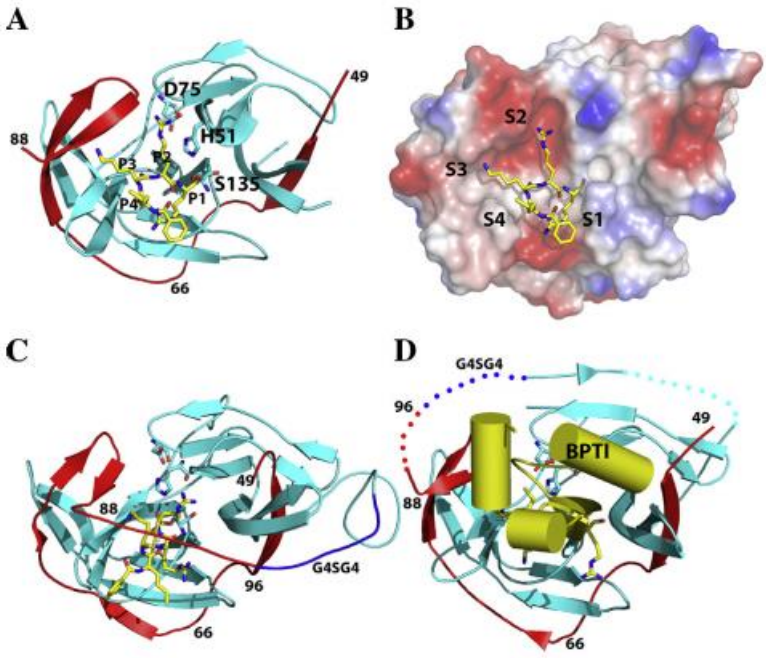

Figure 13: **3D structures of WNV NS2B–NS3pro.** (A): Fold of $NS2B_{47}$NS3pro from WNV. The $NS2B_{47}$ region is shown in red, NS3pro in cyan., inhibitor is yellow (labeled as P1–P2–P3–P4 (PDB ID: 2FP7). (B) Surface view of the substrate binding site of WNV NS2B-NS3pro, S1-S4 coresponded with the P1-P4 of the peptide inhibitor. (C) NMR structure of $NS2B_{49\text{-}96}G_4SG_4$ NS3pro bound to a protease inhibitor in yellow color (BEZ-NLe-Lys-Arg-M9P, PDB ID: 2M9). (D) Crystal structure of WNV $NS2B_{49\text{-}96}G_4SG_4$ NS3pro complexed with inhibitor BPTI (shown in yellow PDB ID: 2IJO). Adapted from [10].

A therapeutic strategy based on inhibiting proteases has been applied successfully for HIV treatment (e. g. efavirenz, navirapene, and delavirdine). Inhibitors prevent virus replication by blocking the HIV-1 protease responsible for producing structural and functional HIV proteins in the host cells [52, 73]. However, the active site of NS3pro is conserved in numerous human serine proteases and lacks key structural features that could be exploited to ensure the specificity and potency of flaviviral inhibitor. Therefore, we consider that interference with the essential NS2B cofactor might be a superior drug discovery strategy compared with targeting of the protease active site [52, 74].

Other protease inhibitors have also been shown to have an effect on flavivirus replication. Temoporfin, a photosensitizer drug approved by the EU for the treatment of squamous cell carcinoma of the head and neck, has been shown to inhibit flavivirus replication via inhibition of the interactions between viral NS2B and NS3 proteins, and is a potent inhibitors for ZIKV. Niclosamide and nitazoxanide which interacst with the active site and blocked it [52, 75, 76]. Besides the standard serin protease inhibitors such as benzamidine, aprotinin, leupeptin, and tosyl-l-lysine chloromethyl ketone, several

peptidic α-keto amide inhibitors were also investigated e. g. telaprevir, grazoprevir, simeprevir and paritaprevir [29, 59, 66].

Viral proteases are proven antiviral targets, and numerous inhibitors have been succesfully developed, however the appropriate inhibitors for TBEV protease have not been discovered yet.

2 Goals

1) Cloning and production of NS3 protease.

2) Purification of recombinant enzyme.

3) Biochemical characterization of the enzyme.

3 Material and Methods

3.1 Material

Plasmid encoding TBEV HYPR fragment involving both NS2 and NS3 proteins was a generous gift from prof. RNDr. Daniel Růžek Ph.D.

3.2 Chemicals and buffers

Table 1: **Chemicals and buffers used for experiments**

Agarose electrophoresis	1x TAE	prepared from 50x stock solution: 242 g Tris, 57.1 mL acetic acid, and 100 mL 0.5M EDTA in ddH_2O
	Agarose gel	1% Agar powder SERVA in 1x TAE
Cell cultivation	S.O.C. medium	2% tryptone, 0.5% yeast extract, 10 mM NaCl, 2.5 mM KCl, 10 mM MgCl2, 10 mM MgSO4, and 20 mM glucose
	Ampicillin plates	5g/L Agar, 10g/L Tryptone, 10g/L NaCl, 5g/L Yeast Extract, 100μg/mL ampicillin
	LB medium	Tryptone (pancreatic digest of casein) 10g/mL, Yeast extract 5g/l, NaCl 5g/l, prepared by suspend 16g LB Broth in 800mL of dH_2O
	Ampicillin	Ampicillin-Na-salt, prepared at 50 mg/mL in ddH_2O
	Chloramphenicol	Chloramphenicol prepared at 50 mg/mL in ethanol
	IPTG	stock solution M is prepared by dissolving Isopropyl β-D-1-thiogalactopyranoside (IPTG) in

		ddH_2O with subsequent sterile filtration of the solution
SDS-PAGE electrophoresis	Lysis buffer	50mM KH2PO4, 400mM NaCl, 100mM KCl, 10% glycerol, 0.5% TritonX-100, 10mM imidazole, pH 7.8
	4x SDS-PAGE sample buffer	4x Laemmli sample buffer stock: 20mL of 0.5M Tris - pH = 6.8, 4g SDS, 20 mL glycerol, 0.1 g of bromophenol blue, H_2O up to 45mL. Addition of 100 µL β-mercaptoethanol into solution SDS-PAGE.
	10x SDS-PAGE transfer buffer	stock: 58.15g Tris, 29.3g glycine, 3.75g SDS
	Fixing solution	60% H_2O, 30% methanol, 10% acetic acid
	Coomassie g-250 Brilliant Blue	0.625g Coomassie g-250 Brilliant Blue, 112.5 mL methanol, 112.5 mL ddH_2O, 25 mL acetic acid
	Resolving gel 12.5%	30% Acrylamide/Bis-acrylamide (37.5:1) = 2.08 mL, H_2O = 1.57 mL, 1.5M Tris pH 8.8 =1.25 mL, 10% SD = 50 µL, 10% APS = 50 µL, TEMED = 5 µL
	Resolving gel 15%	30% Acrylamide (37.5:1) = 2.5 mL, H_2O = 1.15 mL, 1.5M Tris pH 8.8 =1.25 mL, 10% SD = 50 µL, 10% APS = 50 µL, TEMED = 5 µL
	Stacking gel 4%	30% Acrylamide (37.5:1) = 340 mL, H_2O = 1.36 mL, 0.5M Tris pH

		64.8 = 250 mL, 10% SD = 20 µL, 10% APS = 20 µL, TEMED = 2 µL
Western Blot, development solution	TBS-T	10x TBS stock buffer: 60.5g Tris, 87.66g NaCl, pH 7.6; TBS-T prepared by dilution of stock solution to 1x and addition of 1 mL Tween 20
	Blocking solution	prepared from 10x Blocking Reagent Buffer solution:100 mM Maleic acid, 250 mM NaCl, pH 7.5
	1x TBS	10x TBS stock buffer: 60.5g Tris, 87.66g NaCl, pH 7.6
	1x transfer buffer	stock solution: 25 mM Tris, 192 mM glycine, 10% methanol, pH 8.5
Protein production	Lysis buffer	50mM potassium phosphate pH 7.8, 400mM NaCl, 100mM KCl, 10% glycerol, 0.5% triton X-100
IMAC (native purification)	Equilibration buffer	20mM Hepes, 100mM NaCl, pH 7.5
	Elution buffer	20mM Hepes, 100mM NaCl, 1M Imidazol, pH 7.5
IMAC (denature purification)	Equilibration buffer	20mM Hepes, 100mM NaCl, 6M urea, pH 7.5
	Elution buffer	20mM Hepes, 100mM NaCl, 0.5M Imidazol, 6M urea, pH 7.5
IEX	Equilibration buffer	20mM Hepes, pH 7.5
	Elution buffer	20mM Hepes, 1M NaCl, pH 7.5
SEC	Running buffer	20mM Hepes, 100mM NaCl, pH 7.5

3.3 Primer design

Gene Specific primers encoding hydrophilic region of the NS2B and N-terminal (protease) domain of NS3 were designed manually and used to clone both proteins into pETDuet-1 expression vector (Table 2).

Table 2: **Specific primers used for amplification of individual recombinant proteins**

Primer name	**Sequence**	**Coning vector**	**Restriction enzyme**
NS2B_Hypr(duet) _F	CGC**GGATC**CGAGAAAG ATGCAGCTGGTTGC	pETDuet-1	BamHI
NS2B_Hypr(duet) _R	AAGGAAAAAAGC**GGC CGC**TTACATTCTCTCTT CTTTCTCGACCTC	pETDuet-1	NotI
NS3pro__Nterm_Osh_F	TGCTAG**CATATG**TCAG ACTTGGTCTTCTCTGGA CAG	pETDuet-1	Ndel
NS3pro_Chis_duet _R	TACCAT**GATATC**TTAGT CGTGATGATGGTAATGT GATGTCCAGCCCGTGCC	pETDuet-1	EcoRV
NS3pro_duet _R	TACCAT**GATATC**TTATG ATGTCCAGCCCGTGCC	pETDuet-1	EcoRV

Note: (1) The restriction site for each enzyme is highlighted in bold and underlined.

3.4 Polymerase chain reaction (PCR)

3.4.1 Gradient PCR

Gradient PCR was used to determine an optimal annealing temperature of designed primers for each construct. The primers for amplification of N-terminal fragment of NS3 (NS3pro) and the hydrophilic region of NS2B (NS2Bcof) were tested using PPP Master Mix (Top-Bio), which contained a buffer, dNTPs and Taq DNA polymerase. The PCR reaction composed of initial denaturation at 94°C for 1 min and 30 cycles of: denaturation at 94°C for 15 sec, annealing of primers at gradient from 50-60°C for 15 sec and elongation at 72°C for 30 sec. Followed by final extension at 72°C for 7 min and cooling at 12°C.

Concentrations and amounts of PCR components in each reaction mixture is shown in Table 3.

Table 3: **Composition of gradient PCR reaction mixture**

Reagent	**Volume ([µL]**
PPP Master Mix	12,5
R primer (10 µM)	2
F primer (10 µM)	2
Template DNA (50 mg/mL)	0,5
PCR H_2O	8
Final volume	25

The amplified DNA fragments were visualized on 1% agarose gel (SERVA Electrophoresis) stained with Serva DNA Stain Clear G (SERVA Electrophoresis) and using 100 bp DNA Ladder (New England BioLabs,® Inc.) All PCR reactions were conducted in the Biometra Tone Thermal Cycler (Analytik Jena) and pictures taken using G:BOX Chemi, Syngene.

3.4.2 Q5® High- Fidelity DNA Polymerase

Ideal annealing temperature for individual primer pairs were used for amplification of individual genes by Q5® High-Fidelity DNA Polymerase according to manufacturer's recommendations. Briefly initial denaturation at 98°C for 30 sec was followed by 30 cycles of denaturation at 98°C for 10 sec, primer annealing based on previous gradient PCR (NS2Bcof 56°C, NS3pro at 55°C) for 30 sec, elongation at temperature 72°C (15 sec for NS2Bcof and 30 sec for NS3pro), followed by final extension at 72 °C for 2 min. The mixture was kept at 16°C after the process was done. Table 4 shows the concentrations and the amounts of all components for individual reaction.

Table 4: **Composition of Q5® High- Fidelity DNA Polymerase reaction mixtures**

Component	**Volume ([µL]**
Buffer (5x Q5 Reaction Buffer)	10
dNTPs (10 mM)	1
DNA polymerase (Q5 High-Fidelity DNA Polymerase 2U/µL)	0.5
5X Q5 High GC Enhancer	10
R primer (10 µM)	2.5
F primer (10 µM)	2.5
Template DNA (50 mg/mL)	1
PCR H_2O	22.5
Final volume	50

PCR amplicons were mixed with 6x Purple Loading Dye (New England BioLabs,® Inc) and separated according to their size on 1% agarose gel stained with Serva DNA Stain Clear G. Subsequently, target fragments were purified with NucleoSpin Gel and PCR Clean-Up kit (Macherey-Nagel) according to manufacturer´s protocol with exception of using PCR H_2O instead of elution buffer. The DNA concentration was measured with NanoPhotometer Pearl (Implen) and samples were stored at -20°C prior further use.

3.5 Restriction enzyme digestion

DNA fragment encoding NS3pro and NS2Bcof were cloned into pETDuet-1 vector using specific restriction enzymes. The digestion was carried out for 10 min at 37°C followed by the enzyme deactivation for 20 min at 65°C. The composition of reaction mixtures is presented in Table 5. Digested pETDuet-1 vector was further dephosphorylated by adding 2.5 µL rShrimp Alkaline Phosphatase (New England BioLabs,® Inc) and incubating the mixture at 37°C for 30 min followed by inactivation at 65°C for 5 min.

Results of a restriction digest were evaluated by gel electrophoresis using 1% agarose gel stained with Serva DNA Stain Clear G.

Table 5: **Composition of restriction and dephosphorylation reactions**

Reagent	**Restriction Enzyme Double Digestion**	**Dephosphorylation of 5'-ends of DNA using rSAP**
DNA	1 µg	1 µg
10X CutSmart Buffer	5 µL	2 µL
(1) NdeI/EcoRV (2) BamHI/NotI	1 µL /each	
rSAP	-	2.5 µL
ddH2O	up to 50 µL	up to 20 µL
Final volume	50 µL reaction	20 µL reaction

Note: (1) Restriction enzymes designed for NS3 pro that recognize restriction sites in sequences of pETDuet-1 are NdeI and EcoRV.

(2) NotI and BamHI are restriction enzymes for NS2B cofactor and plasmid pETDuet-1.

3.6 Ligation using T4 ligase

Digested amplicons were ligated using T4 DNA ligase (New England BioLabs,® Inc.) at 3:1 molar ratio. The reaction was incubated at 16°C overnight in Biometra TOne followed by heat inactivation at 65°C for 10 min. Table 6 shows the exact composition of ligation reactions.

Table 6: **Composition of ligation reaction into MCS1 and MCS2**

Ligation reaction component – cloning into MCS1	**20 µL reaction**	**Ligation reaction component – cloning into MCS2**	**20 µL reaction**
T4 DNA Ligase Reaction Buffer (10x)	2 µL	T4 DNA Ligase Reaction Buffer (10x)	2 µL
Vector DNA pETDuet-1	50 ng (0.02 pmol) = 5 µL	Vector DNA pETDuet-1	50 ng (0.02 pmol) = 4 µL
Insert DNA NS2B cof	37.5 ng (0.06 pmol) = 0.2 µL	Insert DNA NS3pro	37.5 ng (0.06 pmol) = 1.2 µL
T4 DNA Ligase	1 µL	T4 DNA Ligase	1 µL
ddH_2O	up to 20 µL	ddH_2O	up to 20 µL

3.7 Transformation of NEB® 5-alpha Competent *E. coli* (High Efficiency)

Resulting ligation mixtures were used to transform NEB® 5-alpha *E. coli* cells. Cells were thawed on ice for 20 min, 2 µL of ligation mixture was added and the tube was carefully finger-flicked 4-5 times to mix cells and DNA. The mixture was incubated on ice for 30 min, and subsequently heat-shocked in water bath at 42°C for 30 seconds. After the heat-shock, cells were placed on ice for 2 min. Pre-warmed 250 µL of S.O.C. medium (New England BioLabs,® Inc.) was pipetted into the mixture and vials were shaken at 37°C for 1 hour at 225 rpm in a horizontal position using Eppendorf, InnovaS44i shaker. Next cells were spread on pre-warm LB -ampicillin plates in different volume (50 µL and 150 µL) for visual control of antibiotic selection. The selective plates were incubated overnight at 37°C.

3.8 Colony PCR

Individual colonies were tested for presence of target insert. Colonies were carefully picked by a sterile pipet tip, and the tip was placed in 20 µL of nuclease-free water and pipetted up and down several times. Then the remnants of the mixture on the tip were placed on a new plate marked with numbers defining each colony. Colony PCR was performed according to the Top-Bio PPP Master Mix protocol and composition of reaction mixtures in Table 3 with two differences: A - 1 µL of colony template was added. B - Initial denaturation step at 95°C was increased to 6min, to lyse the cell walls. Aneling primer temperature was based on the gradient PCR. The presence or absence of cloned DNA fragment was verified using 1% agarose gel stained with Serva DNA Stain Clear G together with a positive and negative control.

3.9 Isolation of plasmid and sequence verification

Positive clones from the colony PCR were placed into 4 mL of LB media supplemented with 0.1 mg/mL AMP and the culture was incubated at 37°C and 220 rpm overnight. Next day, the plasmids were isolated utilizing Nucleo-Spin Plasmid mini kit (Macherey-Nagel) following plasmid isolation protocol with elution into 15 µL of water instead of elution buffer. The concentrations of purified plasmids were measured using NanoPhotometer Pearl (Implen), and the presence of the correct gene sequence was verified by sequencing. The same workflow was followed in case maxiprep plasmid isolation. Colonies with correct sequence without any frameshift were placed into 100 mL AMP-LB medium (0.1 mg/mL AMP) and the culture was incubated at 37°C and 220 rpm overnight.

Next day, the plasmids were isolated using Nucleo-Spin Plasmid Xtra midi kit (Macherey-Nagel), measured, and stored prior further work.

3.10 Transformation of BL21 (DE3) Competent *E.coli* and BL21 CodonPlus® competent cells

Plasmids with confirmed correct sequences of NS2Bcof (MSC1) and NS3pro (MSC2) or NS3proH (MSC2) in pETDuet-1 were used to transform the BL21 (DE3) Competent *E.coli* and BL21 CodonPlus® *E.coli* competent cells. The transformation was carried out according to the protocol mentioned in part 3.7 (Transformation to of NEB® 5-alpha Competent *E. coli* (High Efficiency) with one exception – only 1 µL of the purified plasmid (concentration 50 mg/mL) was added to thawed cells. Vials were shaken at 37°C for 1 hour at 225 rpm, subsequently spread over selective plates LB-AMP for BL21 (DE3) or LB-AMP-CAM for CodonPlus® and incubated overnight at 37°C.

3.11 Pilot scale protein production

One colony was picked with a sterile pipet tip and placed into a 50mL centrifuge tube with 10 mL of LB-AMP media (final concentration of 0.1 mg/mL). Culture was incubated overnight at 37°C and 220 rpm in a horizontal shaker. Next day, 0.5 mL of the overnight culture was added to the 10 mL of fresh LB-AMP media containing proper antibiotic (0.1mg/mL AMP for BL21 and 0.1mg/mL AMP, 0.035mg/mL CAM for BL21 CodonPlus®) and incubated at 37°C and 220 rpm until the OD_{600} reached 0.5-0.8 (measured using NanoPhotometer Pearl – by Implen). Once the bacterial culture reached desired OD level, protein production was induced with IPTG (0.1mM final concentration) delivered by Sigma®. Uninduced culture was kept at the same conditions. Afterwards, test cultures were incubated at different temperature 16°C, 20°C, and 30°C and 1mL samples were harvested at defined time interval (Table 7) from both induced and uninduced cultures. Collected samples were centrifuged at maximum speed in a microcentrifuge for 60 sec and pelleted cells were frozen at -20°C.

Subsequently, the pilot protein expression was performed with 1% glucose. Cells grew ON at 37°C and 220 rpm in a horizontal shaker. Next day 10 mL of ON culture was inoculated into 800 mL of LB media containing 1% glucose. Cells were grown until reaching OD_{600} 0.5-0.8. Next the cell culture was spun down at 4500 rpm for 20 min at 4°C. Medium

with glucose was removed and pelleted cells resuspended in fresh LB media. The process of protein production was done as described above.

Table 7: **Temperature and time interval of pilot protein production**

Temperature	Time interval (hour)
16°C	4, 8, 24
20°C	4, 6, 24
30°C	2, 4, 6

3.12 Isolation of soluble and insoluble fraction

The harvested cells from pilot expression experiment were thawed on ice and resuspended in 500 μL of the lysis buffer. Samples were lysed 3 times by consecutive freezing in liquid nitrogen and thawing at 42°C in a heating block. Next, the samples were centrifuged at 15000 rpm at 4°C for 1 min to separate the insoluble and the soluble fraction. The supernatant was removed from the pellet, transferred to a new tube and stored on ice prior to the addition 125 μL of 4x denaturing SDS-PAGE sample buffer. Insoluble proteins were mixed with 500 μL of 1x denaturing SDS-PAGE sample buffer.

3.13 SDS-PAGE Electrophoresis

Denaturing SDS-PAGE electrophoresis was used to separate the cellular proteins using 12,5% and 15% polyacrylamide gels. All samples were incubated at 95°C for 5 min and 3-10 μL of the mixture was loaded on the gel together with 5 μL of 1x Pageruler Protein Ladder #26616 (Thermo Fischer Scientific). The gel run in container with 1x SDS-PAGE running buffer at constant voltage of 100V for 1.5 hour. Upon the run, stacking part of the gel was removed disposed and gels were placed into 20 mL of fixing solution. Next, gels were washed in ddH_2O 2x20 min and stained overnight in 20 mL of Coomassie Brilliant Blue G-250. SDS PAGE result was captured using G:BOX Chemi, Syngene.

3.14 Western Blot

The SDS-PAGE gel was run as described above and the gel was equilibrated for 15 min in 1x transfer buffer. Next the PVDF membrane (Immobilon® - E, Sigma®) was pre-equilibrated in 20 mL of 100% methanol followed by equilibration in 1x transfer buffer and the filter papers were equilibrated also in 1x transfer buffer. The blotting sandwich containing filter paper, membrane and the SDS-PAGE gel has been assembled and the

proteins were transferred to the membrane using Trans Blot Turbo (Biorad). The blotting run on 25V, 1.0A for 30 min. Next the membrane was washed 3x10 min in 1x TBS-T followed by blocking in 3% blocking solution (Qiagen) for 2 hours. After two hours the membrane was washed 3x10 min in TBS-T and incubated with anti-HIS specific antibody (Penta His HRP Conjugate, Qiagen) diluted 1:2000 in a blocking solution for 1 hour. Afterwards, the membrane was washed 2x10 min in 1x TBS-T and 1x10 min in 1x TBS. The specific signal was developed using Clarity Western ECL Substrate Kit (BioRad) and visualized by G:BOX Chemi, Syngene.

3.15 Large scale protein production

The BL21 (DE3) *E.coli* cells were transformed and 50 mL of ON culture was prepared as described in section 3.11. Next day, 10 mL of cell culture was transferred into cultivation bottles prefilled with 800 mL of LB-AMP media (final concentration of 0.1 mg/mL) and incubated in a horizontal shaker at 37°C, 180rpm until OD_{600} reached values between 0.5 to 0.8. At that point, cultures were induced with 0,1mM IPTG and grown according to the specific time interval, shown in Table 7. Finally, the cultures were spun down in a centrifuge at 4°C and 4200 rpm for 20 min. The supernatant was discarded, and the harvested cells were stored at -80°C.

3.16 Protein purification

Harvested cells (pellets from 800mL cultures) were thawed on ice and resuspended in 15 mL of Lysis buffer supplemented with 37.5 µL of RNase-A (50 mg/mL) (Thermo Fisher Scientific, Inc.) and 10 µL of DNase (10 mg/mL) (Sigma®). Cell lysis was performed by passing the cell mixture twice at 10000 psi through the French press (Stansted Fluid Power) and the lysate was clarified by ultracentrifugation at 4°C, 25 000 rpm for 1 hour.

3.16.1 Immobilized metal affinity chromatography

IMAC was done by ÄKTA Pure M2 system (GE Healthcare), fitted with 5 mL HisTrap HP column (GE Healthcare). At first HisTrap HP column and ÄKTA Pure system were washed with double distilled and degassed H_2O for 25 min (5x volume of the column) with a flow rate of 5 mL per min. Next, the HisTrap HP column was equilibrated with 5CV of degassed and filtered equilibration buffer followed by 5CV of elution buffer (degassed and filtered) and again 5CV of equilibration buffer.

The sample – supernatant from the centrifugation – was loaded on the column using sample pump, at a flow rate of 1 mL per min. The flow-through fraction was collected when UV started to rise. When the sample was loaded, the system was equilibrated in the equilibration buffer until the UV dropped to the baseline. Next, the equilibration buffer was changed to 5% elution buffer to remove unspecifically bound proteins and the eluted fraction was collected. Subsequently, the gradient of elution buffer was set to increase to 100% over 20 min at flow rate of 1mL/min. Once the UV started to rise, 1 mL fractions were collected using the fraction collector. After the purification, the system was washed using elution buffer (5CV), equilibration buffer (5CV), followed by H_2O (5CV) and kept in 20% ethanol. Collected fractions were analysed on SDS-PAGE gel (15% gel) followed by Western Blot analysis. Fractions containing protein of interest were pooled prior next purification step.

3.16.2 Anion exchange chromatography

AEC was done using ÄKTA Pure M2 system (GE Healthcare) fitted with the 5mL HiTrap Q HP column (GE Healthcare). The system was washed and equilibrated as described above with degassed and filtered AEC equilibration and elution buffers. To reduce the NaCl concentration in pooled protein fractions the loaded sample was diluted using HEPES buffer without any NaCl. Next, the sample was loaded to the column and eluted using gradient 0-100% of elution buffer over 20 min at 1mL/min flowrate. Once the UV started to rise 1mL fractions were collected using fraction collector. Purification result was checked using SDS-PAGE (15% gel) and Western Blot (15% gel).

3.16.3 Size exclusion chromatography

SEC was performed by ÄKTA Pure system (GE Healthcare) fitted with 25mL Superdex 75 Increase 10/300 GL column (GE Healthcare). The column was washed with 2 CV of H_2O followed by 2 CV of running buffer. The sample was concentrated to 3.886 mg/mL and 500 μL was loaded manually by syringe. The purification ran at flow rate of 0.3 mL per min. Volume 0.3 mL fractions were collected as soon as the protein peak appeared. Finally, the purity of the protein was validated using SDS-PAGE and Western blot (15% gel). The concentration of purified protein was measured using NanoPhotometer Pearl (Implen).

3.17 Enzyme assays

To verify the proteolytic activity of the enzyme the fluorescence substrate ZRR-AMC (Bachem) was used. All experiments were done in technical triplicates. The assay was conducted in a black 96-well plate using various buffers as described below. The final reaction volume of 100 μL contained 4 μM recombinant protease, and 200 μM substrate. The fluorescence signal was measured at excitation 360 nm, emission 460 nm, 30°C per 1 min for either 30 or 15 min using either Synergy H1 (BioTek) or Infinite® 200 PRO (Tecan) readers.

3.17.1 Effect of pH

NS2Bcof-NS3proH activity was assayed over broad pH range 5.5-11 (increments 0.5 pH, 50mM buffer). The pH range was covered using various buffers with the appropriate buffer capacity: MES buffer (5.5-7 pH), HEPES buffer (7-8 pH), Tris-HCl buffer (8-9 pH), and CAPS buffer (9-11 pH). Each buffer pH was prepared separately at RT.

3.17.2 Effect of glycerol

Glycerol dependence was examined by varying concentrations (0%, 10%, 20%, 30%, 40%, 50%) of glycerol in reaction mixture. The glycerol was mixed in 8.5 Tris-HCl buffer and the enzyme assay was performed as described in chapter 3.17.

3.17.3 Effect of Ionic strength

The effect of increasing ionic strength on enzyme activity was tested under various amounts concentrations of NaCl (0mM-25-50-100-150-200mM). The defined amount of NaCl was added into 8.5 Tris-HCl buffer and the proteolytic activity of NS3pro was examined as described above.

3.17.4 Enzyme kinetics

NS3pro kinetic parameters such as Km and Kcat were tested using ZRR-AMC substrate under the optimal processing conditions which were examined previously (pH 8.5 Tris-HCl, 30% glycerol). Final reaction volume of 100 μL included 4 μM recombinant protease and various concentrations of substrate (0 μM – 2M). The assay was conducted at 30 °C and the fluorescence signal at ex. 460 nm em. 640nm was recorded every minute. The results were graphed according to Michaelis-Menten kinetics.

$$v = \frac{v_{\max} \cdot [s]}{k_m + [s]}$$

Then we calculated the binding affinity constant Km and the reaction rate Kcat.

$$k_{cat} = \frac{v_{\max}}{[E]}$$

4 Results

Genes encoding either NS2Bcof or NS3pro have been cloned into pETduet-1 allowing simultaneous production of two proteins in *E. coli* expression system. NS2Bcof have been cloned into MSC1 with an N-terminal His tag. NS3pro have been cloned into MCS2 with (NS3proH) or without (NS3pro) C terminal his tag, which was added to the protein to ensure the affinity purification. Picture 14 shows generated constructs.

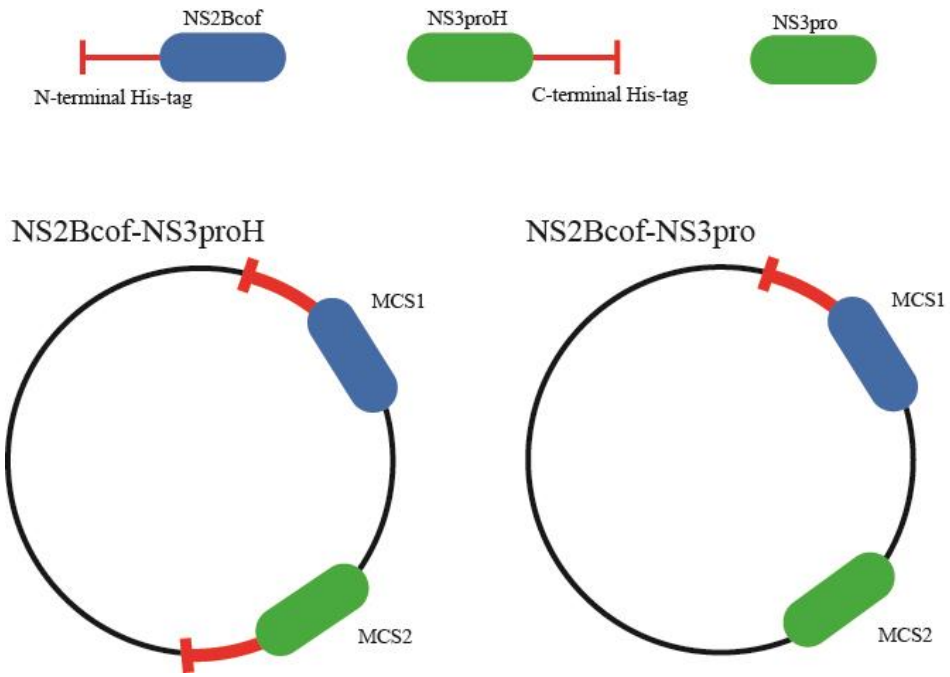

Figure 14: **Scheme of NS2Bcof-NS3pro, NS2Bcof-NS3proH constructs.**

4.1 Gradient PCR

Gradient PCR have been used to determine an optimal annealing temperature of designed primers. Temperature gradient spanning from 50-60°C was applied resulting in an ideal annealing temperature of 55°C for all primer pairs.

4.2 Cloning of NS2B, NS3pro

All constructs were amplified with Q5 High-Fidelity Polymerase, which possesses $3' \rightarrow 5'$ exonuclease activity to ensure ultra-low error rate. Presence of the NS2Bcof (147 bp) and both NS3 constructs (570 bp, 588 bp) was verified by 1% agarose gel electrophoresis (Figure 15). PCR amplicons were purified from the gel yielding the DNA concentration

of 57.4 ng/µL for NS2Bcof, 128 ng/µL for NS3pro, and 139 ng/µL for NS3proH, respectively.

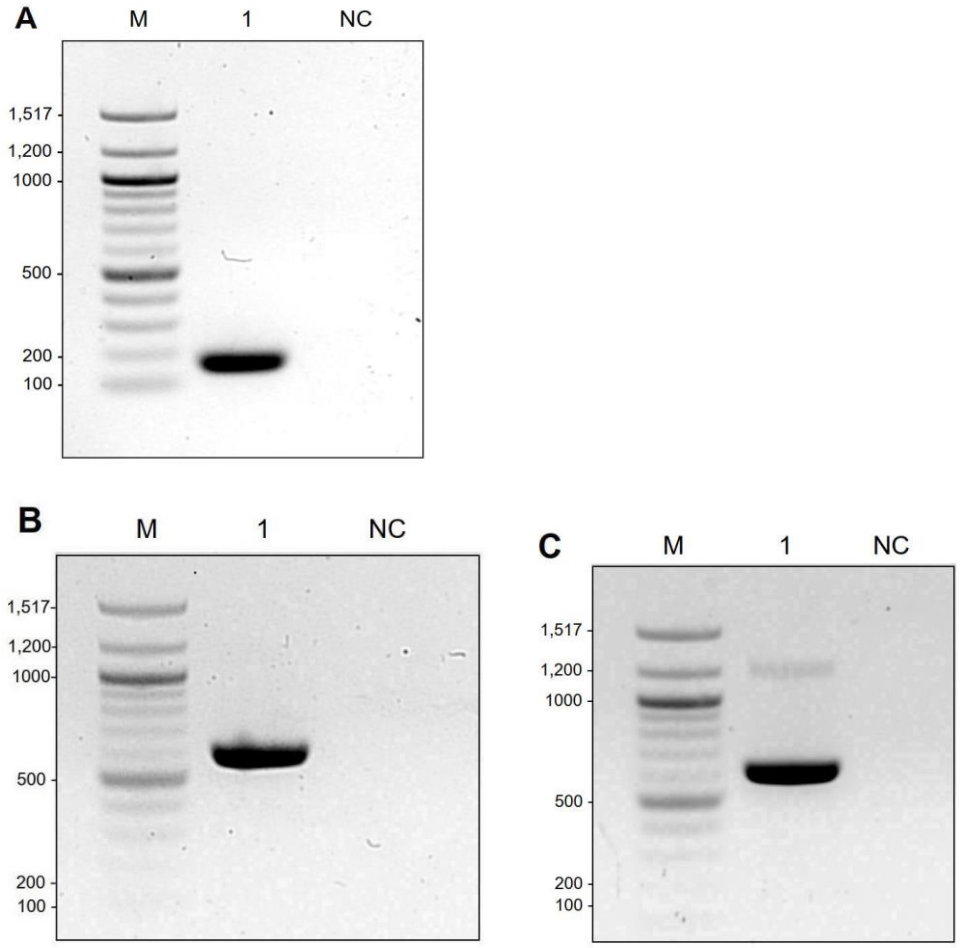

Figure 15: **Gel electrophoresis of gradient PCR product NS2Bcof, NS3pro, NSA3proH**. (A):1 – sample NS2Bcof, (B): 1 – sample NS3pro, (C): 1 – sample NS3proH. M – 100bp DNA Ladder (New England BioLabs,®), NC – negative control containing no DNA template.

4.2.1 Insertion of NS2Bcof into MCS1

NotI and BamHI restriction enzymes were used to insert NS2Bcof into MSC1 of pETDuet-1. Digested DNA was purified and ligated at 3:1 molar ration using T4 DNA ligase. Resulting ligation mixture was used to transform NEB® 5-alpha Competent E. coli cell.

Next day, the presence of pETDuet-1 carrying NS2cof in MCS1 was verified by colony PCR (Figure 16). We tested 12 colonies, 5 of them had visible band on 1% gel, which ran around 200bp corresponding to the expected size of NS2Bcof.

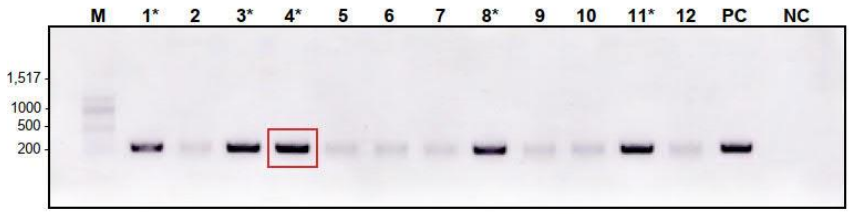

Figure 16: **Colony PCR analysis NS2Bcof.** M – 100 bp DNA Ladder (New England BioLabs,®). PC – positive control (DNA template of Hypr-7). NC – negative control (tip touch on LB plate). Individual clones numbered by 1-12. Samples marked with an asterisk were sent for sequencing. Sample four (marked with a red frame) was used for further experiments.

Five clones have been used to prepare minipreps and plasmid isolation. Isolated plasmids were measured and sent for sequence verification to SEQme company. All sequenced plasmids carried the correct insert without any frameshift. Colony carrying plasmid number four was used for maxiprep preparation and isolated plasmid was used for further work.

4.2.2 Insertion of NS3pro and NS3proH into MCS2

Cloning of both NS3pro and NS3proH into MCS2 was done using NdeI and EcoRV restriction enzymes. Digested amplicons and pETduet-1 carrying NS2Bcof in MCS1 were mixed in 3:1 molar ration and ligated using T4 DNA ligase. Competent cells NEB® 5-alpha were transformed by ligation mixture and grown overnight. Next day presence of either NS3pro or NS3proH gene fragment was verified by colony PCR. In total 3 out of 24 colonies resulted in a band of size about 500 bp corresponding to NS3pro (Figure 17) and 20 out of 24 colonies were tested positive for presence of NS3proH (Figure 18).

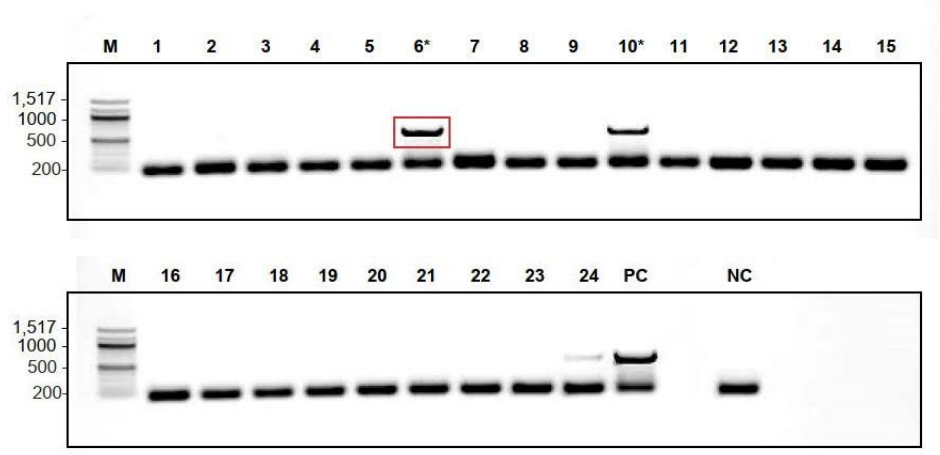

Figure 17: **Colony PCR analysis NS3pro.** M – 100 bp DNA Ladder (New England BioLabs,®), PC – positive control (DNA template of Hypr-7). NC – negative control (tip touch on LB plate). Samples 1-24 – NSS3pro.

Samples marked with an asterisk were sent for sequencing. The sample six marked with a red frame was used to make maxiprep.

Two colonies (6 and 10) were used to prepare minipreps and plasmid isolation. Isolated plasmids were measured and send to SEQme company. Both colonies with correct sequence did not contain any errors. Colony number six was used for maxiprep preparation and isolated plasmid was used for further work.

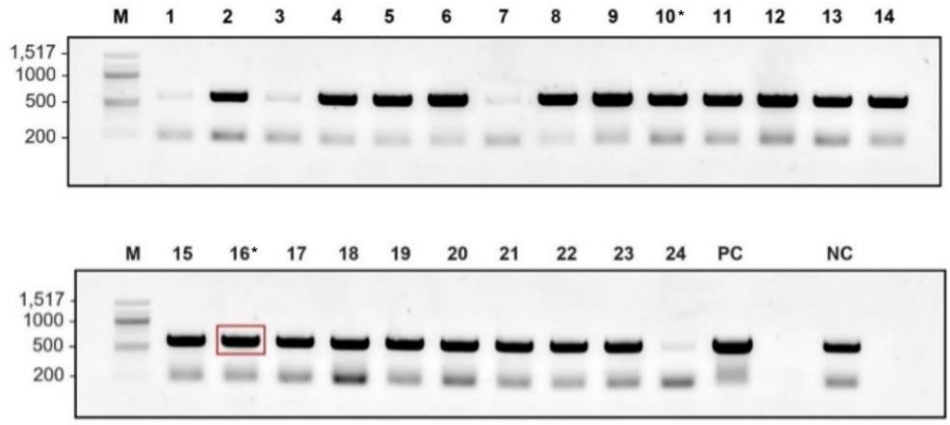

Figure 18: **colony PCR analysis NS3proH**. M – 100 bp DNA Ladder (New England BioLabs,®), PC – positive control (DNA template of Hypr-7). NC – negative control (tip touch on LB plate). Samples 1-24 – NSS3proH. Samples marked with an asterisk were sent for sequencing. The sample sixteen (marked with a red frame) was used to make maxiprep.

Two clones (10 and 16) have been chosen for plasmid isolation, measured and send for sequence verification to SEQme. Sequencing results confirmed that both samples contain the correct insert without any frameshift. Sample 16 was used to make a maxipreps and isolated plasmid was stored for further work.

4.3 Pilot protein production

The pilot expression was performed to determine optimal condition for recombinant protein production in two *E. coli* competent cell lines and under various conditions. E. *coli* BL21 (CodonPlus®) competent cells were grown in LB-AMP-CAM at 37°C until they reached the 0.64 OD_{600} (NS2Bcof-NS3pro) 0.69 OD_{600} (NS2Bcof-NS3proH). The protein production was then induced by addition of 1mM IPTG and the cell culture was incubated at 16°C, 20°C, or 30°C. Protein production was monitored by sampling 1 mL of the culture at various time intervals 20°C (4h, 6h, 24h), 30°C (2h, 4h, 6h), 16°C (4h, 8h, 24h). All samples were pelleted, and the cell pellet was stored at -20°C prior further use. The soluble

and insoluble fraction was prepared from all taken samples and analysed by SDS-PAGE under reducing conditions. Unfortunately, none of tested conditions yielded a detectable amount of recombinant protein that could be visualized by Coomassie Brilliant Blue G-250. Western blot analysis using Anti-His antibody was done, but no significant result was observed (data are not shown).

Because the production of either NS2Bcof-NS3pro or NS2Bcof-NS3proH was not detected in the BL21 (CodonPlus®), another cell line of *E. coli* BL21 (DE3) was tested. Recombinant protein production was tested at two different temperatures 16°C and 30°C for both constructs. The process was the same as in case of BL21 CodonPlus. BL21 (DE3) Competent *E. coli* were grown in LB-AMP (at 37°C until they reached the OD_{600} – NS2Bcof-NS3proH = 0.68 OD_{600}, NS2Bcof-NS3pro = 0.71 OD_{600}). Then each culture was induced by 1mM IPTG. Protein production was monitored at defined time interval for 16°C (4h, 8h, 24h) and 30°C (2h, 4h, 6h). After isolation of soluble and insoluble fraction and all samples were analysed via SDS-PAGE electrophoresis.

Estimated molecular weight of NS2Bcof-NS3pro is 27.6 kDa (20,3 kDa NS3pro, 7.3 kDa NS2Bcof) and of NS2Bcof-NS3proH is 28.5 kDa, NS3proH 21.2 kDa, NS2Bcof 7.3 kDa). SDS-PAGE showed no significant protein production in soluble and insoluble part at 16°C (Figure 19) for both NS3pro and NS3proH.

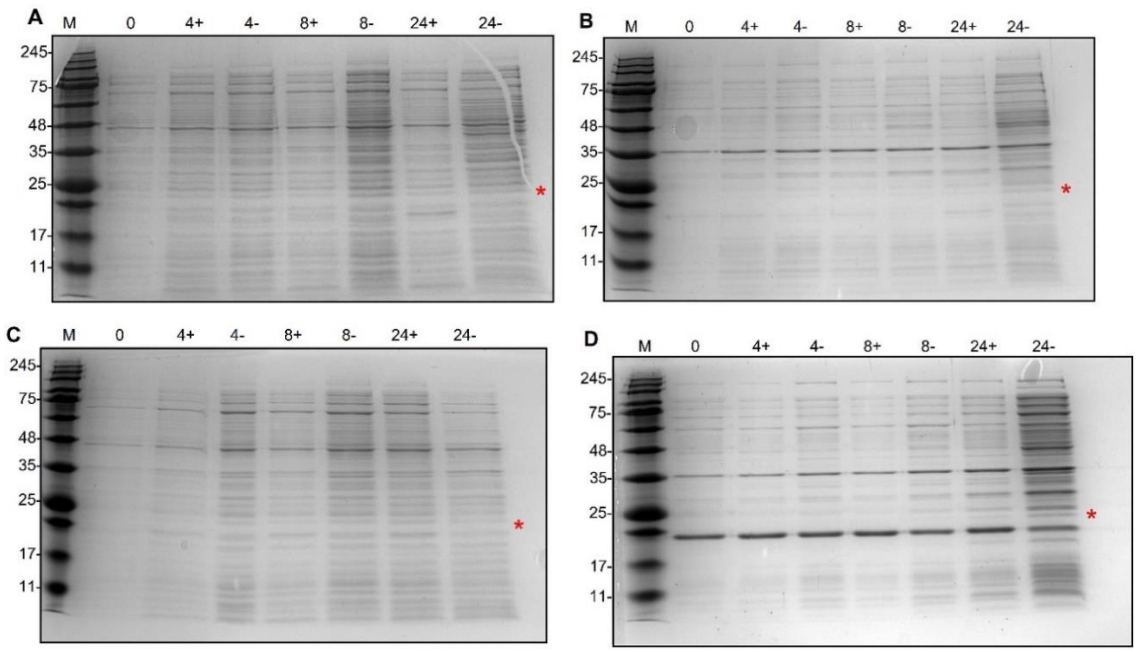

Figure 19: **SDS-PAGE analysis of protein expression BL21 (DE3) Competent *E.coli* at 16°C**. (A): soluble fraction NS2Bcof-NS3pro, (B): insoluble fraction NS2Bcof-NS3pro, (C): soluble fraction NS2Bcof-NS3proH, (D): insoluble fraction NS2Bcof-NS3proH. M – PageRuler Prestained Protein Ladder (Thermo Fischer). - indicates uninduced culture while + indicates induced culture, each number stands for an hour of collection of the sample after the induction. * correspond to the expected area of the NS3pro.

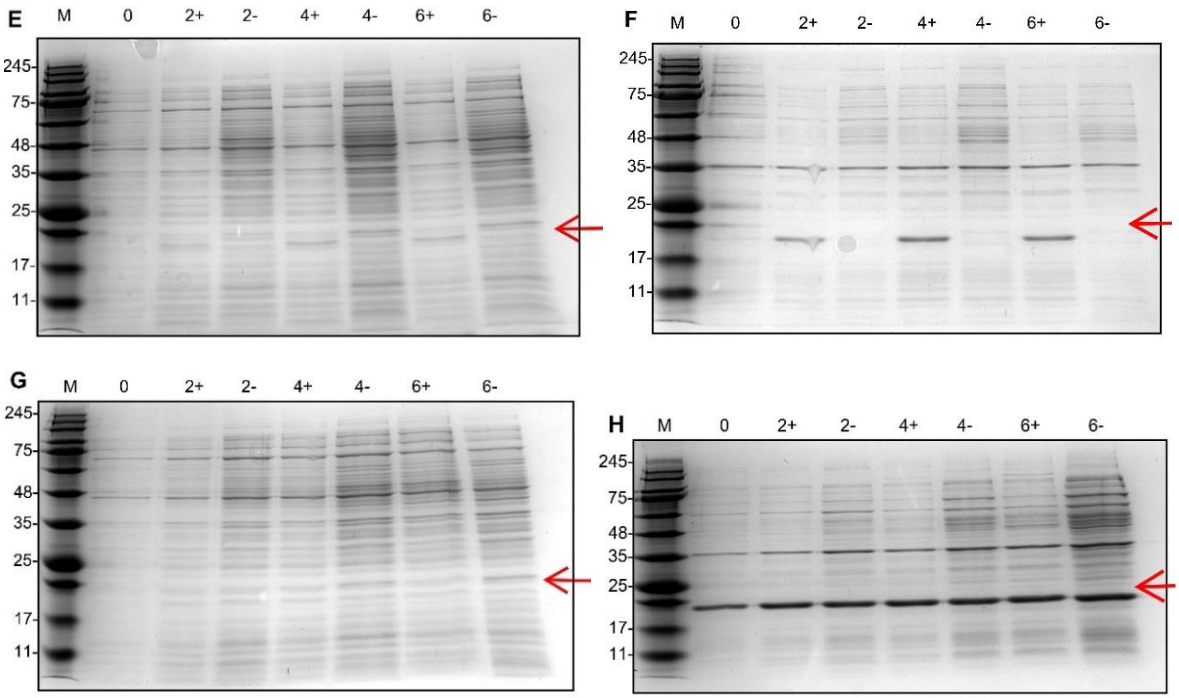

Figure 20: **SDS-PAGE analysis of protein expression BL21 (DE3) Competent *E.coli* at 30°C-** (E): soluble fraction NS2Bcof-NS3pro, (F): insoluble fraction NS2Bcof-NS3pro, (G): soluble fraction NS2Bcof-NS3proH, (H): insoluble fraction NS2Bcof-NS3proH. M – PageRuler Prestained Protein Ladder (Thermo Fischer). - indicates uninduced culture while + indicates induced culture, each number stands for an hour of collection of the sample after the induction. * correspond to the expected area of the NS3pro.

Low intensity bands corresponding to the expected size of (NS2Bcof-NS3pro, NS2Bcof-NS3proH) were detected in the soluble fraction of cells growing at 30°C (Figure 20). The presence of correct protein in these fractions was verified by Western blot (in both insoluble and soluble fractions using Anti-His antibody (Figure 21).

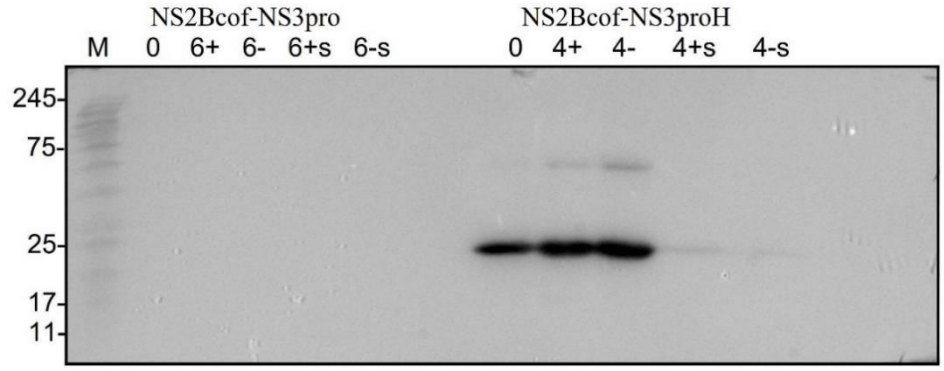

Figure 21: **Western blot BL21 (DE3) Competent *E.coli* at 30°C, NS2Bcof-NS3pro and NS2Bcof-NS3proH**. M – PageRuler Prestained Protein Ladder (Thermo Fischer), + sign indicates induced culture, s – indicates soluble fraction.

Start with saying that there was signal also in uninduced fraction, which is due to the leaky promotor, and we wanted to check, if the protein is not somehow harming the cells. From this reason we grew the cells in the presence of 1% glucose prior induction, replace the medium and performed the pilot expression. We used again BL21 (DE3) (for NS2Bcof-NS3pro and NS2Bcof-NS3proH) and time interval 16°C (4h, 8h, overnight) and 30°C (2h, 4h, 6h), however we did not observe any improvement (data not shown).

Since the Western Blot confirmed the presence of NS2Bcof-NS3proH in the soluble fraction of *E. coli* BL21 cells, we decided to perform the large-scale protein production. Large scale protein production was done based on the results from pilot expression - NS2Bcof-NS3proH (30°C, 4 hours) NS2Bcof-NS3pro (30°C, 6 hours).

Table 8: **Summary of all pilot expression experiments and evaluation**

Competent cell + insert	**Inducer**	**Antibiotics resistance**	**Temperature**	**Time interval (hour)**	**Protein production**	
BL21 CodonPlus® +NS2BNS3H	IPTG	AMP, CAM	20 °C	4, 6, 24	soluble	-
					insoluble	-
BL21 CodonPlus® +NS2B-NS3	IPTG	AMP, CAM	20 °C	4, 6, 24	soluble	-
					insoluble	-
BL21 CodonPlus® +NS2B-NS3H	IPTG	AMP, CAM	30 °C	2, 4, 6	soluble	-
					insoluble	+
BL21 CodonPlus® + NS2B-NS3	IPTG	AMP, CAM	30 °C	2, 4, 6	soluble	-
					insoluble	-
BL21 CodonPlus® +NS2B-NS3H	IPTG	AMP, CAM	16 °C	4, 8, 24	soluble	-
					insoluble	-
BL21 CodonPlus® + NS2B-NS3	IPTG	AMP, CAM	16 °C	4, 8, 24	soluble	-
					insoluble	-
BL21 (DE3) +NS2B-NS3H	IPTG	AMP	16 °C	4, 8, 24	soluble	-
					insoluble	-
BL21 (DE3) + NS2B-NS3	IPTG	AMP	16 °C	4, 8, 24	soluble	-
					insoluble	-
BL21 (DE3) +NS2B-NS3H	IPTG	AMP	30 °C	2, 4, 6	soluble	+
					insoluble	+
BL21 (DE3) + NS2B-NS3	IPTG	AMP	30 °C	2, 4, 6	soluble	+
					insoluble	-
BL21 (DE3) +NS2B-NS3H + glucose	IPTG	AMP	16 °C	4, 8, 24	soluble	-
					insoluble	-
BL21 (DE3) + NS2B-NS3 + glucose	IPTG	AMP	16 °C	4, 8, 24	soluble	-
					insoluble	-

Competent cell + insert	Inducer	Antibiotics resistance	Temperature	Time interval (hour)	Protein production	
BL21 (DE3) +NS2B-NS3H + glucose	IPTG	AMP	30 °C	2, 4, 6	soluble	+
					insoluble	+
BL21 (DE3) + NS2B-NS3 + glucose	IPTG	AMP	30 °C	2, 4, 6	soluble	+
					insoluble	-

Note: (1) - indicate low or no production of recombinant protein

(2) + indicates sufficient recombinant protein production.

(3) NS2B-NS3H is an aberration for NS2Bcof-NS3proH.

(4) NS2B-NS3 is an aberration for NS2Bcof-NS3pro.

4.4 Large scale protein production

Based on the results of SDS-PAGE and Western blot the best conditions were selected (temperature and time intervals for both constructs) and large scale recombinant protein production started. NS2Bcof-NS3proH protein was produced at 30°C for 4 hours (1mM IPTG induction at OD_{600} 0.71), while NS2Bcof-NS3pro protein was produced at 30°C for 6 hours (1mM IPTG induction at OD_{600} 0.73). Upon the production, each cell culture was spun down at 4°C and 4200 rpm for 20 min, and cell pellets were stored at -80°C prior purification. SDS-PAGE and WB analysis were performed to verify the presence of recombinant protein in the culture (data not shown).

4.5 Immobilized metal affinity chromatography

IMAC purification was used to purify both histidine-tagged recombinant proteins. The His-tag has a high affinity for metal ions and binds strongly to the IMAC column. Most other proteins in the lysate will not bind to the resin or bind only weakly. Cells were resuspended in lysis buffer containing protease inhibitor, supplemented 37.5µL with of RNase-A (50 mg/mL) and 15µL of DNase (10 mg/mL). Cells were lysed two times at 10000 psi by the French press (Stansted Fluid Power) and the resulting lysate was centrifuged (25000 rpm, 4°C) in ultracentrifuge to pellet the insoluble fraction. Next, the supernatant (40 mL) was loaded on the HisTrap column and purified via IMAC. The recombinant protein was eluted via gradient of elution buffer (Figure 22). 1 mL fractions were collected and analysed on 15% gel SDS-PAGE and Western blot 15% gel (Figure 23). Both NS3pro proteins were

purified by IMAC, however the NS2Bcof-NS3proH with added His-tag showed higher purification efficiency and was used for further experiments.

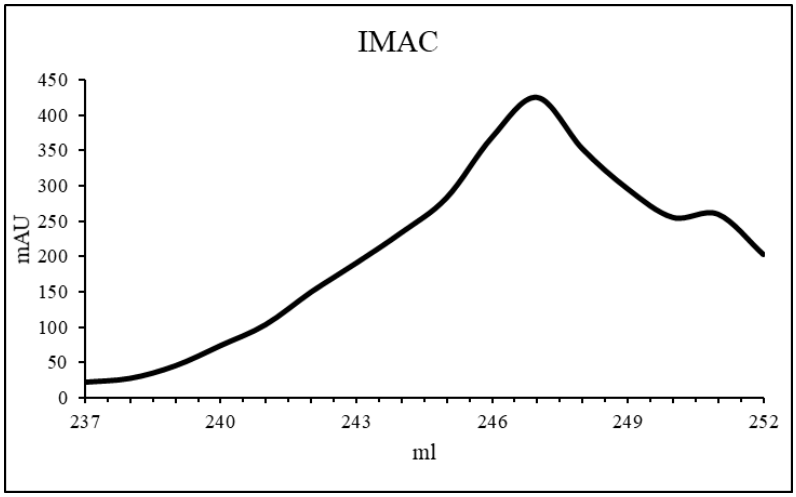

Figure 22: **Immobilized metal affinity** chromatography. NS2Bcof-NS3proH chromatogram with HisTrap column. Fraction collection 2-16.

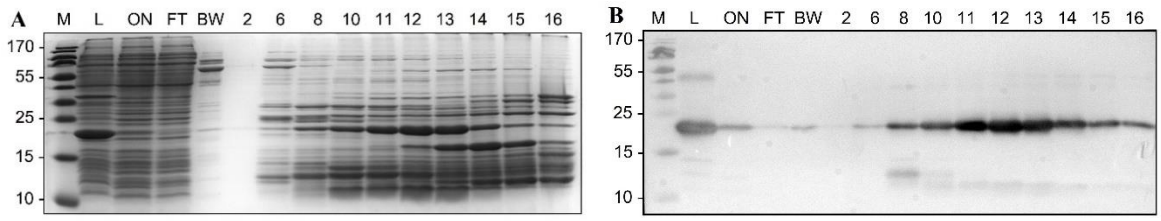

Figure 23: **SDS-PAGE analysis and Western Blot analysis of IMAC native purification of the NS2Bcof-NS3proH**. (A): SDS-PAGE analysis, (B): Western blot analysis. M – PageRuler Prestained Protein Ladder #26616 (Thermo Fischer), L – cell lysate, ON – injected supernatant, BW – 5% fraction collected when the column washed with 5% elution buffer, 2-16 fractions collected during gradient elution.

4.6 Anion exchange chromatography

IMAC fractions (8-15) were pooled together and diluted by AEC equilibration buffer (1:10) to reduce the amount of the salt in the sample. Diluted sample was loaded onto HiTrap Q HP column and purified via AEC. NS3proH protein was eluted using NaCl gradient and fractions analysed on SDS-PAGE (Figure 24). As seen in Figure 24, peak fractions (5-8) contained a significant amount of protein, while a small peak fraction 9-15 contained some other proteins from *E. coli*.

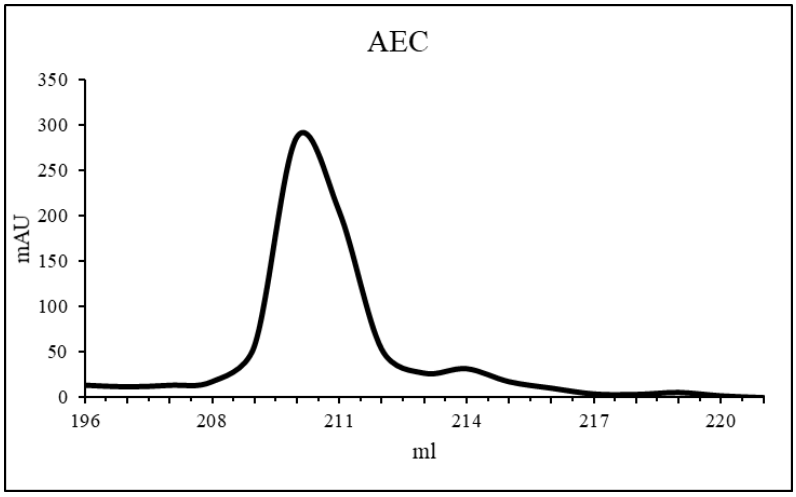

Figure 24**: Anion exchange chromatography. NS2Bcof-NS3proH chromatogram with HiTrap column**. Fraction collection 1-15.

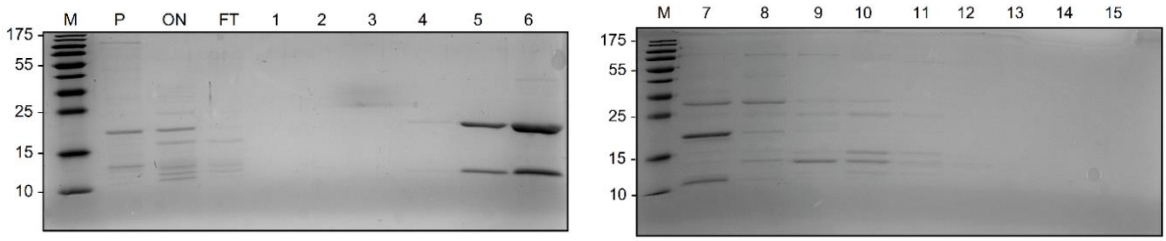

Figure 25: **Chromatogram of AEC native purification and SDS-PAGE analysis of the purification of the NS2Bcof-NS3proH.** M – PageRuler Prestained Protein Ladder #26616 (Thermo Fischer), P – cell pellet from IMAC, ON – injected supernatant from IMAC, FT – flow-through fraction, 1-15 fractions collected during gradient elution.

4.7 Size exclusion chromatography

AEC fractions 5, 6, 7 were pooled together and used for final purification step using SEC. Samples were concentrated using amicon filter (3K cat off) and loaded onto Superdex75 column. The purification was done at flow rate of 0.3 mL/min (Figure 26) and resulting fraction were analysed by SDS-PAGE and by Western blot (Figure 27).

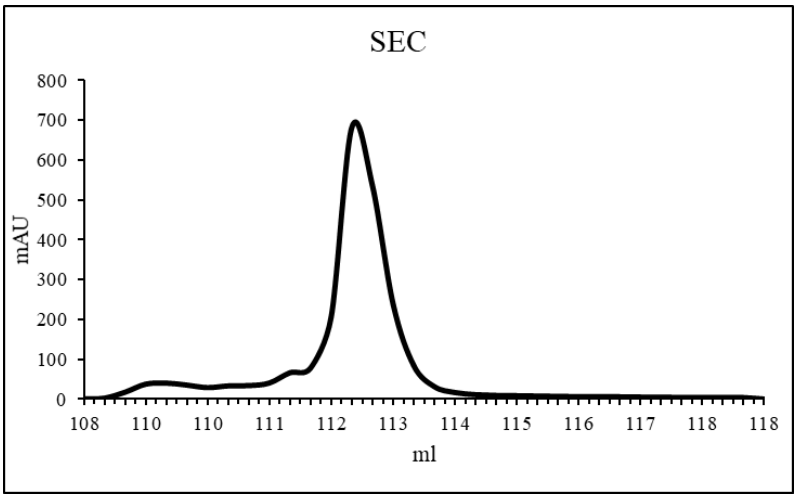

Figure 26: **Size exclusion chromatography. NS2Bcof-NS3proH chromatogram with Superdex75 column.** Fraction collection A5-B8.

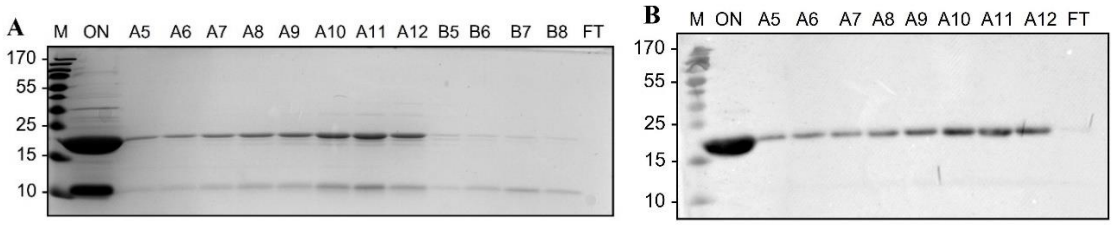

Figure 27: **SDS-PAGE analysis and Western Blot analysis of SEC purification of the NS2Bcof-NS3proH**. (A): SDS-PAGE analysis, (B): Western blot analysis. M – PageRuler Prestained Protein Ladder #26616 (Thermo Fischer), ON – samples from AEC purification, A5-B8 fractions collected during running buffer elution, FT – flow throw from the buffer exchange by amicon.

Besides Western blot, the presence of NS2Bcof-NS3proH was verified by mass spectrometry using our department facility. After the conformation, protein concentration in fractions A5-A12 was measured and the protein was aliquoted and stored at -80 °C for the purpose of protease assays.

4.8 Enzymatic assays

Several enzyme assays were performed to characterize the enzymatic activity of recombinant NS2Bcof-NS3proH. Proteolytic activity was monitored under a variety of assay conditions, culminating in an optimum set of pH value, ionic strength, and amount of glycerol.

Enzymatic characterization of the recombinant NS3 serine protease was assayed against ZRR-AMC substrate. The assay was conducted in a black 96-well plate with a final reaction volume of 100 μL containing buffer, 4 μM recombinant protease, and 200 μM

substrate. The fluorescence signal was measured at 460/640 nm, 30°C per 1 min for 30/15 min.

Firstly, the effect of pH on enzymatic activity was assayed over a wide pH range from pH 5.5-11 using a variety of buffers suitable for each range. The assay was done in technical and biological triplicates and the fluorescence signal was measured every minute for 30 min (Figure 28).

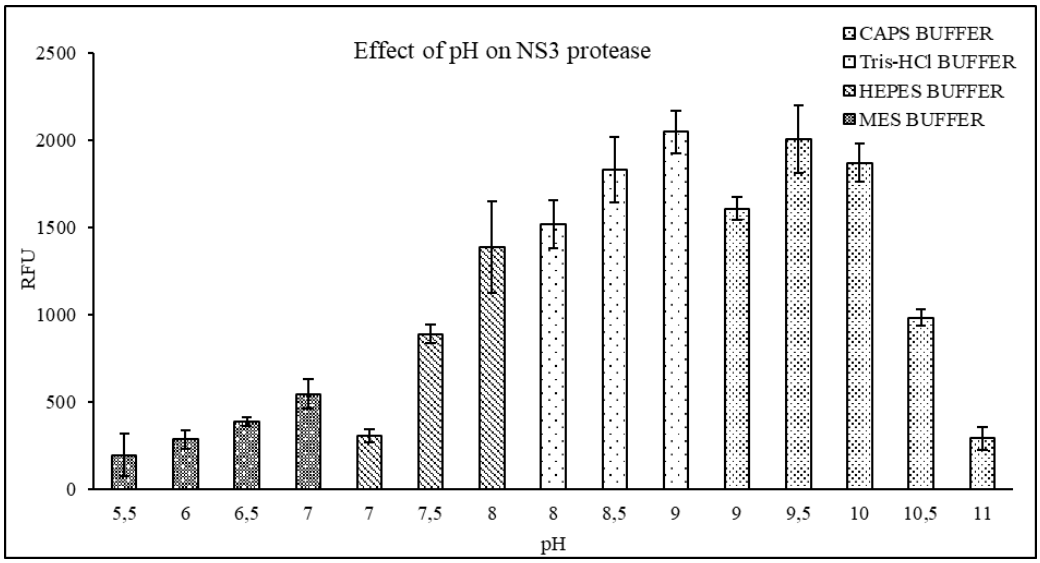

Figure 28: **Enzymatic characterization of NS2Bcof-NS3proH domain from TBEV, effects of pH**. The range of pH 5.5-11, increments 50 mM, in a final volume 100 µL, measured at 15 minutes.

Low and high pH does not appear to be suitable for protease activity. The NS3pro has a bell-shaped pH optima, peaking around pH 9. For further studies we decided to use pH 8.5 Tris-HCl (1829 RFU, SD±189), which is not on the edge of the buffering capacity.

Secondly, the effect of glycerol on enzymatic activity was tested of varying glycerol concentration (0-10-20-30-40-50%). The assay was done in technical and biological triplicates and the fluorescence signal was measured every minute for 30 min. However, we did not observe any substantial effect of the glycerol on enzymatic activity (Figure 29).

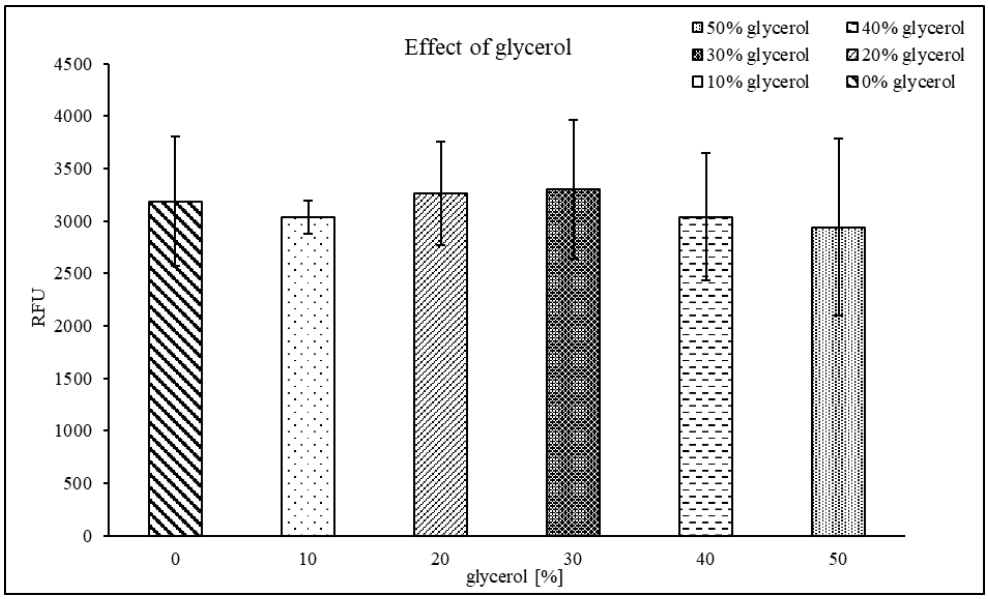

Figure 29: **Enzymatic characterization of NS2Bcof-NS3proH domain from TBEV, effects of glycerol.** Glycerol dependence of increasing glycerol content 0-50% (10% increments), in a final volume of 100 μL, measured at 15 minutes.

It has been described previously that 30% glycerol enhances catalytic processing of WNV NS3 protease [82]. Based on this study, we decided to perform the experiments in the presence of 30% glycerol (3303 RFU, SD±658).

Thirdly, the effect of increasing ionic strength on enzymatic activity was tested by adding NaCl (0-200mM NaCl). The assay was done in technical and biological triplicates and the fluorescence signal was measured every minute for 30 min. Figure 30 shows ionic strength dependence at time 15 min. Our data suggests that NaCl concentration in the range of 0-150mM does not have any substantial effect of the protease activity, but when increased to 200mM we did observe an inhibition. To further confirm the finding, new assays with higher NaCl concentration shall be performed.

As we did not observe any effect of ionic strength on protease activity within the 0-150mM range, we performed the assays without any NaCl.

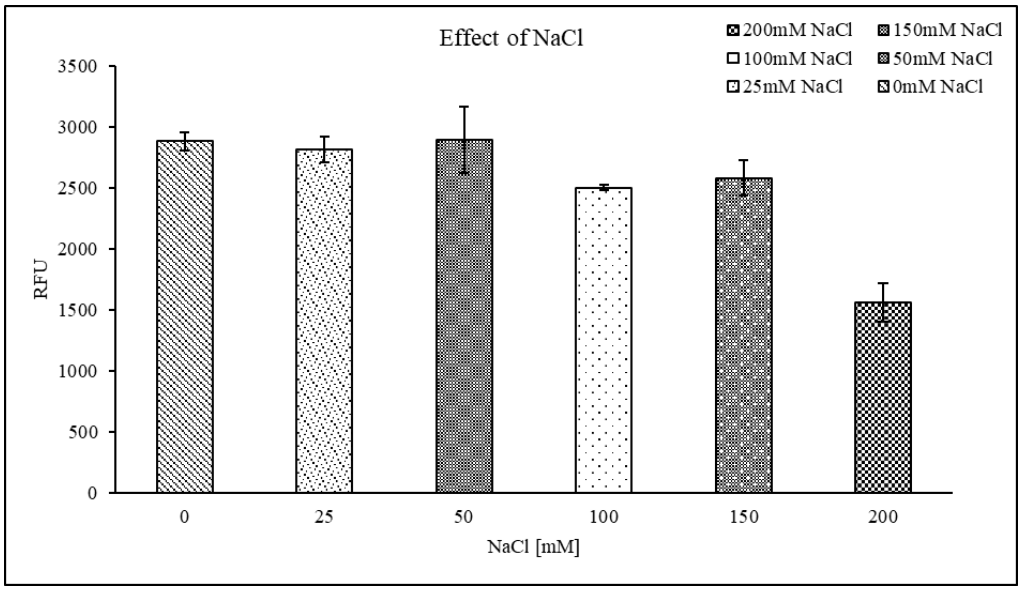

Figure 30: **Enzymatic characterization of NS2Bcof-NS3proH domain from TBEV, effects of ionic strength.** Increasing ionic strength and the protease activity, measured at 15 minutes.

Finally, the enzyme kinetic was assayed. NS2Bcof-NS3proH was tested for its capacity to cleave ZRR-AMC substrate under the optimal processing conditions which were examined previously (pH 8.5 Tris-HCl (50 mM), 30% glycerol), with a final reaction volume of 100 µL. Reaction includes 4 µM recombinant protease and substrate concentrations ranging from 0 µM – 2M. The results were graphed according to Michaelis-Menten kinetics (Figure 31).

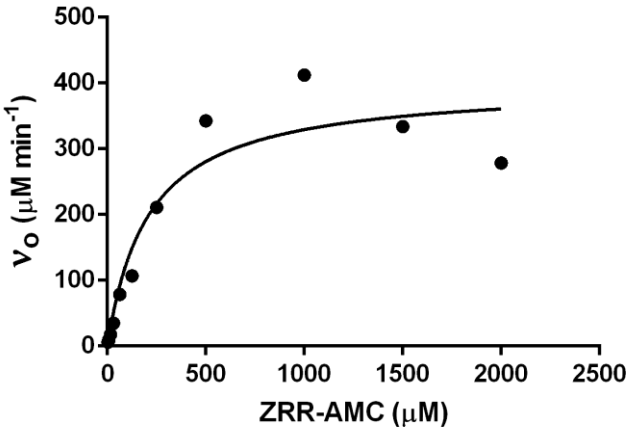

Figure 31: **Characterization of protease domain from TBEV NS3. Km determination of ZRR-AMC substrate,** measured at 15 min.

The kinetics parameter of the protease was determined, Km for NS2Bcof-NS3proH TBEV is 210.2 µM ± 78.74 SD and Kcat 99.61 s^{-1} ± 10.29.

5 Discussion

TBEV NS3 serine protease is involved in proteolytic processing of viral polyprotein and it has a crucial role in viral replication. In this study we produced, purified, and biochemically characterized a catalytically active NS2Bcof-NS3pro enzyme complex. Results summarized in the thesis will be used for further characterization of TBEV NS3pro enzyme and could lay the foundation for the development of antiviral treatment.

NS3 protease requires its NS2B cofactor not only for its catalytic activity, but also for the proper folding and solubility [78]. The presence of NS2B membrane anchors substantially hampers the recombinant production of NS3pro. However, it has been shown that only the cofactor region of NS2B pro is necessary for proper folding and activity of the protease [52, 54]. Several papers describing the NS3pro from various flaviviruses have been published and authors mostly connect the core region of NS2B to the NS3pro using short aa linker and produced fusion protein. However, these constructs differ in many details e.g. type and length of the linker, length of NS2B domain, and some of these differences have been shown to have an impact on protease properties [66]. In our approach, we decided to produce unlinked ("native") form of NS2Bcof-NS3pro using pETDuet-1 expression vector, which has two multiple cloning sites, and allows for simultaneous production of two proteins in competent *E. coli* cells. Despite using various cell lines and production conditions, most of the produced protein was found in the insoluble pellet fraction. This suggests that the protein may not be folded correctly, and it is stored inside the cells in the form of inclusion bodies. This has been also the case of DNV NS3 protease [79]. The formation of inclusion bodies is quite common phenomena for *E. coli* expression system. However, the recombinant proteins can be recovered by denaturing purification followed by various refolding techniques [80]. This process can be quite successful, but in our case, we need to refold two proteins and optimize the conditions not only allowing for correct protein folding, but also for their proper interaction. Despite the low production level of recombinant protein in the soluble fraction, we decided to rather increase the volume of cell culture than to optimize the refolding conditions.

Both covalent and noncovalent NS2B-NS3 protease complexes from several flaviviruses have been biochemically tested *in vitro* and shown various activities. Our aim was a biochemical characterization of the TBEV protease in the form of unlinked complex, which has been shown to have higher protease activity and binds substrate with greater affinity than more frequently used linked NS2B-NS3 constructs [81].

To characterize its enzymatic properties, we monitored the protease activity at various conditions. NS2Bcof-NS3proH was assayed over a wide pH range from pH 5.5–11.0 (50 mM) using a variety of buffers suitable for each pH value. Our data clearly show that lower (5.5-7) and high (11) pH values are not suitable for protease activity. This can be because such extreme values (low and high) can cause the denaturation of the enzyme. The enzyme is active over a broad pH range from pH 7.5 to pH 10, peaking at pH 9. This finding is supported by another studies, which defined the activity of recombinant proteases to be at neutral/basic pH values using covalently linked construct [82]. Kim and colleagues (2013) [83] reported that unlinked NS2B-NS3pro from DNV2 has high activity at pH 7 suggesting that Gly-rich linker may influence the protease activity [83]. The effect of linker on the enzyme activity was analysed by Shannon and colleagues (2016) [84] for DNW NS3 protease. They reported that the effect of pH on enzymatic activity of the unlinked and glycine-linked proteases followed the trend, with activity peaking at pH 9 for both constructs. Interestingly, the unlinked complex shown minimal activity at pH 7, and preferred the basic pH value. This discrepancy between Kim and colleagues (2013) and Shannon and colleagues (2016) have not been explained yet but may be a result of the differences in the protein expression, as well as addition of His-tag. The similarity in optimal pH between unlinked and linked NS2B-NS3 protease excludes the possibility that the incorporated Gly-rich-linker is artificially modifying the enzyme in a way that effects proteolytic processing at physiological pH value. The pH optimum around pH 9.0 is above the physiological value and may indicate an increased pH in the subcellular membranous compartment in which the proteolytic activity takes place [84]. Nevertheless, as the protease has not been examined in more details within a cellular context, the reason for hight pH optimum of NS2B-NS3pro need to be further investigated.

Subsequently, the effect of glycerol on protease activity was tested. Glycerol has been shown to enhance catalytic processing of Dengue NS3 protease and attribute to minimize the enzyme aggregation [79]. We therefore examined the effect of varying glycerol concentrations (0 –50%). As the result we obtained a linear concentration dependence on glycerol but increasing glycerol concentration and increasing viscosity of aqueous solution limited the protease assay and increased the error rate from pipetting.

After we characterized the optimal pH and concentration of glycerol, we decided to examine the effect of ionic strength on enzymatic activity by adding various concentrations of NaCl (0-200mM). The results indicate that higher ionic strength (above 200mM) inhibits the proteolytic processing of the substrate. NaCl might conceivably be detrimental for the

activity by competing with substrate and water molecules for occupancy of the substrate binding active site, thus inhibiting substrate processing. Another possibility explaining the inhibition of substrate processing has been published by Tyndall and colleagues (1999) [85]. NaCl is known for its preference of α-helicity in peptides, and thus may alter conformational equilibria of substrates in solution, rendering them less recognizable to the protease. NS3 protease only recognizes its substrate and inhibitor molecules in an extended β-strand conformation. β-sheets are fundamentally different in that their arrays of β-strands utilize most of the peptide backbone amides in inter-strand hydrogen bonded networks, and thus are not exposed or available for interactions with proteases. The results show that β-sheets tend to be resistant to proteolytic procession [85].

Previous studies have shown that specific serine protease inhibitors such as benzamidine, aprotinin, leupeptin, and tosyl-l-lysine chloromethyl ketone inhibit WNV protease at 100μM concentration [86]. We tested the inhibitory effect of aprotinin (160 μM) in comparison to an active an inactivated enzyme under same condition. We observed no protease activity upon adding the inhibitor, however further study shall be performed to examine the inhibitor profile.

Based on biochemical characterization of the enzyme, the enzyme kinetics of NS2Bcof-NS3proH was determined. The protease assay was performed at 30°C, 15 min, pH 8.5 (50mM), 30% glycerol with (0-2000 μM) ZRR-AMC substrate. Km for NS2B-NS3proH TBEV is 210.2 μM and Kcat 99.61 s^{-1}. The higher Kcat might indicated, that protease processed faster, more substrates get turned over in one second. A low Km might indicate higher affinity, it means the reaction can reach half of Vmax in a smaller number of substrate concentration. We used for kinetics characterization ZRR-AMC substrate with two cleavage sites (P1, P2) and past studies have shown shorter substrates (di-, tri- and tetrapeptide) can be processed more efficiently by recombinant flavivirus proteases. It might be due to easier access and binding to the active site, in comparison with the longer substrates. Most of the protease assay used longer substrate and different set up conditions, from this reason it is difficult to find close studies and compare our finding. Although, Nitche and colleagues (2014) [66] performed the enzyme kinetics of DNV protease with substrate Bz-RR AMC and obtained Km 247 μM, compare to 210.2 μM (Km) for the TBEV NS2Bcof-NS3proH, this might confirm a higher affinity to substrate, but further studies are required for detailed characterization of enzyme properties.

Detailed biochemical characterization together with atomic-resolution crystal structures of TBEV NS3pro are essential for design of specific NS2B-NS3 inhibitors. Combinations

of structure-based mutagenesis, protein enzymatic activity study *in vitro* and X-ray crystallography can gain us more insights into this multi-functional protein. Challenging aspect in the search for potent, selective, antiviral drug that interfere with multi-functional protein NS3 is the design of appropriate assays for druggable sites that are relevant for viral replication *in vivo*. The development of such drugs which target the viral serin protease and do not negatively influence the host immune system requires a more information about both NS3 structure and function. Development of appropriate inhibitors (or activators) of the NS3 protease for TBEV should also be of great benefit in combating other infections caused by flaviviruses

6 Conclusion

Cloning of TBE NS3 protease was performed using pETDuet-1 vector. This plasmid has two cloning sites and allows production of two recombinant proteins in one cell without the need of additional vector. Using various cell lines and production conditions, we optimized the recombinnat production of NS2Bcof-NS3pro. The best conditions for recombinant production of NS2Bcof-NS3proH in the soluble fraction have been found when using BL21 (DE3) Competent *E.coli* and performing the protein production at 30°C for 4 hours.

The combination of IMAC, AEC and SEC have been applied to purify the recombinant protein. Our data also show that the addition of His-tag to the C terminus of NS3pro increase the yield of purified protein.

The recombinant NS2Bcof-NS3pro enzyme was successfully produced and tested for its protease activity. Biochemical characterazion of the enzyme provided us with first information about the activity properties of this enzyme. The effect of glycerol, ionic strenght and pH range on enzymatic activity was monitored and the conditions for optimized enzyme assay were defined as follow: 8.5 pH, 30% glycerol, 0 nM NaCl. The Kinetic constats of NS2Bcof-NS3pro have beed identified: Km 210.2 μM ± 78.74 SD and Kcat 99.61 s^{-1} ± 10.29.

7 References

[1] Pulkkinen, L. I. A,, Butcher, S. J., Anastasina, M. (2018). Tick-Borne Encephalitis Virus: A Structural View. Viruses, 10(7), 350.

[2] Lindquist, L.,Vapalahti, O. (2008): Tick-Borne Encephalitis. Lancet, 371, 1861−71.

[3] Růžek, D., Danielová, V., Daniel, M., Chmelík, V., Chrdle, A., Pzadiora, P., Pry-mula R., Salát, J., Žampachová, E. (2015): Klíšťová encefalitida. Praha Grada Publishing, s. 19-137. ISBN 978-80-247-5305-8.

[4] Ginsburg, A. S., Meghani, A., Halstead, S. B., & Yaich, M. (2017). Use of the live attenuated Japanese Encephalitis vaccine SA 14–14–2 in children: A review of safety and tolerability studies. Human Vaccines & Immunotherapeutics, 13(10), 2222–2231.

[5] Mansfield, K. L., Johnson, N., Phipps, L. P., Stephenson, J. R., Fooks, A. R., & Solomon, T. (2009). Tick-borne encephalitis virus - a review of an emerging zoonosis. Journal of General Virology, 90(8), 1781–1794.

[6] Pierson, T. C., Diamond, M. S. (2012): The Complex Structure and Biology of Flaviviruses. Current Opinion in Virology, 2, 168−75.

[7] Ginsburg, A. S., Meghani, A., Halstead, S. B., & Yaich, M. (2017). Use of the live attenuated Japanese Encephalitis vaccine SA 14–14–2 in children: A review of safety and tolerability studies. Human Vaccines & Immunotherapeutics, 13(10), 2222–2231.

[8] Grard, G., Moureau, G., Charrel, R.N., Lemasson, J.J., Gonzalez, J.P., Gallian, P., Gritsun, T.S., Holmes, E.C., Gould, E.A., de Lamballerie, X. (2007): Genetic characterization of tick-borne flaviviruses-´- New insights into evolution, pathogenetic determinants and taxonomy. Virology, 361, 80–92

[9] Mansfield, K. L., Johnson, N., Phipps, L. P., Stephenson, J. R., Fooks, A. R., & Solomon, T. (2009). Tick-borne encephalitis virus - a review of an emerging zoonosis. Journal of General Virology, 90(8), 1781–1794.

[10] Heinze, D.M., Gould, E.A., Forrester, N.L. (2012):Revisiting the clinal concept of evolution and dispersal for the tick-borne flaviviruses by using phylogenetic and biogeographic analyses. Journal of Virology, 86, 8663–8671.

[11] Dobler, G. (2010): Zoonotic Tick-Borne Flaviviruses. Veterinary Microbiology, 140, 221−8.

[12] Heinze, D.M., Gould, E.A., Forrester, N.L. (2012): Revisiting the clinal concept of evolution and dispersal for the tick-borne flaviviruses by using phylogenetic and biogeographic analyses. Journal of Virology, 86, 8663–8671.

[13] Bogovic, P.; Strle, F. Tick-borne encephalitis: A review of epidemiology, clinical characteristics, and management. World Journal of Clinical Cases, 3, 430.

[14] Wallner, G., Mandl, C.W., Kunz, C., Heinz, F.X. (1995): The flavivirus 3'-noncoding region: Extensive size heterogeneity independent of evolutionary relationships among strains of tick-borne encephalitis virus. Virology, 213, 169–178.

[15] Kollaritsch, H., Chmelík, V., Dontsenko, I., Grzeszczuk, A., Kondrusik, M., Usonis, V., Lakos, A. (2011): The current perspective on tick-borne encephalitis awareness and prevention in six Central and Eastern European countries: Report from a meeting of experts convened to discuss TBE in their region. Vaccine, 29, 4556–456.

[16] Whitehead, S. S., Durbin, A. P., Pierce, K. K., Elwood, D., McElvany, B. D., Fraser, E. A., Carmolli, M. P., Tibery, C. M., Hynes, N. A., Jo, M., Lovchik, J. M., Larsson, C. J., Doty, E. A., Dickson, D. M., Luke, C. J,; Subbarao, K., Diehl, S. A., Kirkpatrick, B. D. (2017):In a Randomized Trial, the Live Attenuated Tetravalent Dengue Vaccine TV003 Is Well-Tolerated and Highly Immunogenic in Subjects with Flavivirus Exposure Prior to Vaccination. PLoS Neglected Tropical Disseases, 11(5).

[17] Kuhn, R. J., Zhang, W., Rossmann, M. G., Pletnev, S. V., Corver, J., Lenches, E., Jones, T., Chipman P. R., Strauss G. E., Baker T. S., Strauss, J. H. (2002): Structure of dengue virus: implications for flavivirus organization, maturation, and fusion. Cell 108, 717–725.

[18] Füzik, T., Formanová, P., Růžek, D., Yoshii, K., Niedrig, M.; Plevka, P. (2018): Structure of tick-borne encephalitis virus and its neutralization by a monoclonal antibody. Nature Commun, 9, 436.

[19] Mukhopadhyay, S, Kim, B.S., Chipman, P.R., Rossmann, M.G., Kuhn, R.J. (2003): Structure of West Nile virus. Science, 302, 248.

[20] Wang, X., Li, S.H., Zhu, L., Nian, Q.G., Yuan, S., Gao, Q., Hu, Z., Ye, Q., Li, X.F., Xie, D.Y., Shaw, N., Wang, J., Walter, T. S., Huiskonem J. T., Fry, E. E., Qin, CH-F., Stuart, D., Rao, Z. (2017): Near-atomic structure of Japanese encephalitis virus reveals critical determinants of virulence and stability. Nature Commun, 8, 14.

[21] Lindenbach, B.D., Murray, C.L., Thiel, H. J., Rice, C.M. (2007): Flaviviridae: The Viruses and Their Replication. Fields Virology, 5, 1101-1133.

[22] Zhang, Y., Kostyuchenko, V.A., Rossmann, M.G. (2007): Structural analysis of viral nucleocapsids by subtraction of partial projections. Journal of Structural Biology, 157, 356–364.

[23] Malygin, A.A., Bondarenko, E.I., Ivanisenko, V.A., Protopopova, E.V., Karpova, G.G., Loktev, V.B. (2009): C-terminal fragment of human laminin-binding protein contains a receptor domain for Venezuelan equine encephalitis and tick-borne encephalitis viruses. Biochemistry, 74, 1328–1336.

[24] Plevka, P., Battisti, A. J., Junjhon, J., Winkler, D. C., Holdaway, H. A., Keelapang, P. Rossmann, M. G. (2011): Maturation of flaviviruses starts from one or more icosahedrally independent nucleation centres. EMBO Reports, 12(6), 602–606.

[25] Kostyuchenko, V.A., Xiao, C., Bowman, V.D., Battisti, A.J., Yan, X., Chipman, P.R., Baker, T.S., Van Etten, J.L., Rossmann, M.G. (2009) An icosahedral algal virus has a complex unique vertex decorated by a spike. PNAS, 106, 11085–11089.

[26] Corver, J., Ortiz, A., Allison, S.L., Schalich, J., Heinz, F.X., Wilschut, J. (200): Membrane fusion activity of tick-borne encephalitis virus and recombinant subviral particles in a liposomal model system. Virology, 269, 37–46.

[27] Stiasny, K., Heinz, F.X. (2004): Effect of membrane curvature-modifying lipids on membrane fusion by tick-borne encephalitis virus. Journal of Virology, 78, 8536–8542.

[28] Prasad, V.M., Miller, A.S., Klose, T., Sirohi, D., Buda, G., Jiang, W., Kuhn, R.J., Rossmann, M.G. (2017): Structure of the immature Zika virus at 9 Å resolution. Nature Structural & Molecular Biology, 24, 184–186.

[29] Muller, D. A., & Young, P. R. (2013). The flavivirus NS1 protein: Molecular and structural biology, immunology, role in pathogenesis and application as a diagnostic biomarker. Antiviral Research, 98(2), 192–208.

[30] Crabtree, M.B., Kinney, R.M., Miller, B.R. (2005): Deglycosylation of the NS1 protein of dengue 2 virus, strain 16681: construction and characterization of mutant viruses. Archives of Virology, 150, 771–786.

[31] Rathore, A. P. S., Paradkar, P. N., Watanabe, S., Tan, K. H., Sung, C., Connolly, J. E., Loe, J., Ooi, E. E., Vasudevan, S. G. (2011). Celgosivir treatment misfolds dengue virus NS1 protein, induces cellular pro-survival genes and protects against lethal challenge mouse model. Antiviral Research, 92(3), 453–460.

[32] Barrows, N. J., Campos, R. K., Liao, K.-C., Prasanth, K. R., Soto-Acosta, R., Yeh, S.-C., Schott-Lerner,G., Pompon, J., Sessions, O. M., Bradrick, S. S., Garcia-Blanco, M. A. (2018). Biochemistry and Molecular Biology of Flaviviruses. Chemical Reviews, 118(8), 4448–4482.

[33] Zhang, Y., Corver, J., Chipman, P.R., Zhang, W., Pletnev, S.V., Sedlak, D., Baker, T.S., Strauss, J.H., Kuhn, R.J., Rossmann, M.G. (2003): Structures of immature flavivirus particles. EMBO Journal, 22, 2604–2613.

[34] Bogovic, P., Strhle, F. (2015). Tick-borne encephalitis: A review of epidemiology, clinical characteristics, and management. World Journal of Clinical Cases, 3(5), 430.

[35] Rastogi, M., Sharma, N., & Singh, S. K. (2016). Flavivirus NS1: a multifaceted enigmatic viral protein. Virology Journal, 13(1).

[36] Kurz, M., Stefan, N., Zhu, J., & Skern, T. (2012). NS2B/3 proteolysis at the C-prM junction of the tick-borne encephalitis virus polyprotein is highly membrane dependent. Virus Research, 168(1-2), 48–55.

[37] Li, X.-D., Deng, C.-L., Ye, H.-Q., Zhang, H.-L., Zhang, Q.-Y., Chen, D.-D., Zhang, P.T., Shi, P.-Y., Yuan Z.-M., Zhang, B. (2016). Transmembrane Domains of NS2B Contribute to both Viral RNA Replication and Particle Formation in Japanese Encephalitis Virus. Journal of Virology, 90(12), 5735–5749.

[38] Yau, W.-L., Nguyen-Dinh, V., Larsson, E., Lindqvist, R., Överby, A. K., & Lundmark, R. (2019). Model System for the Formation of Tick-Borne Encephalitis Virus Replication Compartments without Viral RNA Replication. Journal of Virology, JVI.00292-19.

[39] Liu, W. J., Chen, H. B., Wang, X. J., Huang, H., & Khromykh, A. A. (2004). Analysis of Adaptive Mutations in Kunjin Virus Replicon RNA Reveals a Novel Role for the Flavivirus Nonstructural Protein NS2A in Inhibition of Beta Interferon Promoter-Driven Transcription. Journal of Virology, 78(22), 12225–12235.

[40] Shiryaev, S.A., Chernov, A.V., Aleshin, A.E., Shiryaeva, T.N., Strongin, A.Y. (2009): NS4A regulates the ATPase activity of the NS3 helicase: A novel cofactor role of the non-structural protein NS4A from West Nile virus. Journal of General Virology, 90, 2081–2085.

[41] Khasnatinov, M. A., Tuplin, A., Gritsun, D. J., Slovak, M., Kazimirova, M., Lickova, M., Gritsun, T. S. (2016). Tick-Borne Encephalitis Virus Structural Proteins Are the Primary Viral Determinants of Non-Viraemic Transmission between Ticks whereas Non-Structural Proteins Affect Cytotoxicity. PLOS ONE, 11(6), e0158105.

[42] Zmurko, J., Neyts, J., & Dallmeier, K. (2015). Flaviviral NS4b, chameleon and jack-in-the-box roles in viral replication and pathogenesis, and a molecular target for antiviral intervention. Reviews in Medical Virology, 25(4), 205–223.

[43] McLean, J. E., Wudzinska, A., Datan, E., Quaglino, D., & Zakeri, Z. (2011). Flavivirus NS4A-induced Autophagy Protects Cells against Death and Enhances Virus Replication. Journal of Biological Chemistry, 286(25), 22147–22159.

[44] Best, S.M. (2017): The many faces of the flavivirus NS5 protein in antagonism of type I interferon signaling. Journal of Virology, 91(16).

[45] Chambers, T. J., Weir, R. C., Grakoui, A., McCourt, D. W., Bazan, J. F., Fletterick, R. J., & Rice, C. M. (1990). Evidence that the N-terminal domain of nonstructural protein NS3 from yellow fever virus is a serine protease responsible for site-specific cleavages in the viral polyprotein. Proceedings of the National Academy of Sciences, 87(22), 8898–8902.

[46] Li, K., Phoo, W. W., & Luo, D. (2014). Functional interplay among the flavivirus NS3 protease, helicase, and cofactors. Virologica Sinica, 29(2), 74–85.

[47] Fairman-Williams, M. E., Guenther, U. P., Janowsky, E. (2010): SF1 and SF2 helicases: family matters. Current Opinion in Structural Biology, 20, 312-324.

[48] Matusan, A. E., Pryor, M. J., Davidson, A. D., & Wright, P. J. (2001). Mutagenesis of the Dengue Virus Type 2 NS3 Protein within and outside Helicase Motifs: Effects on Enzyme Activity and Virus Replication. Journal of Virology, 75(20), 9633–9643.

[49] Frick DN. Helicases as antiviral drug targets. (2003): Drug News & Perspectives, 16(6), 355–362.

[49] Wang, C.-C., Huang, Z.-S., Chiang, P.-L., Chen, C.-T., & Wu, H.-N. (2009). Analysis of the nucleoside triphosphatase, RNA triphosphatase, and unwinding activities of the helicase domain of dengue virus NS3 protein. FEBS Letters, 583(4), 691–696.

[50] Benarroch, D., Selisko, B., Locatelli, G. A., Maga, G., Romette, J.-L., & Canard, B. (2004). The RNA helicase, nucleotide 5′-triphosphatase, and RNA 5′-triphosphatase activities of Dengue virus protein NS3 are Mg2+-dependent and require a functional Walker B motif in the helicase catalytic core. Virology, 328(2), 208–218.

[51] Clum, S., Ebner, K. E., Padmanabhan, R. (1997): Cotranslational membrane insertion of the serine proteinase precursor NS2B-NS3(Pro) of dengue virus type 2 is required for efficient in vitro processing and is mediated through the hydrophobic regions of NS2B. Journal of Biological Chemistry, 272(49), 30715–30723.

[52] Luo, D., Vasudevan, S. G., & Lescar, J. (2015). The flavivirus NS2B–NS3 protease–helicase as a target for antiviral drug development. Antiviral Research, 118, 148–158.

[53] Robin, G., Chappell, K., Stoermer, M. J., Hu, S.-H., Young, P. R., Fairlie, D. P., & Martin, J. L. (2009). Structure of West Nile Virus NS3 Protease: Ligand Stabilization of the Catalytic Conformation. Journal of Molecular Biology, 385(5), 1568–1577.

[54] Erbel, P., Schiering, N., D'Arcy, A., Renatus, M., Kroemer, M., Lim, S. P., Yin, Z., Keller, T. H., Vasudevan, S. G., Hommel, U. (2006): Structural basis for the activation of flaviviral NS3 proteases from dengue and West Nile virus. Nature Structural & Molecular Biology, 13: 372-373.

[55] Noble, C. G., She, C. C., Chao, A. T., Shi, P. Y. (2012): Ligand-bound structures of the dengue virus protease reveal the active conformation. Journal of Virology, 86: 438-446.

[56] Gu, M., & Rice, C. M. (2009). Three conformational snapshots of the hepatitis C virus NS3 helicase reveal a ratchet translocation mechanism. Proceedings of the National Academy of Sciences, 107(2), 521–528.

[57] Chambers, T. J., Nestorowicz, A., Amberg, S. M., Rice, C. M. (2008): Mutagenesis of the yellow fever virus NS2B protein: effects on proteolytic processing, NS2B-NS3 complex formation, and viral replication. Journal of Virology 67, 6797-6807.

[58] Noble, C. G., Chen, Y.-L., Dong, H., Gu, F., Lim, S. P., Schul, W., Wang, W. S., Shi, P.-Y. (2010). Strategies for development of dengue virus inhibitors. Antiviral Research, 85(3), 450–462.

[59] Su, X.-C., Ozawa, K., Qi, R., Vasudevan, S. G., Lim, S. P., & Otting, G. (2009). NMR Analysis of the Dynamic Exchange of the NS2B Cofactor between Open and Closed Conformations of the West Nile Virus NS2B-NS3 Protease. PLOS ONE Neglected Tropical Diseases, 3(12), e561.

[60] Gouvea ,I. E., Izidoro, M. A., Judice, W. A., Cezari, M. H., Caliendo, G., Santagada, V., Santos, C. N., Queiroz, M. H., Juliano, M. A., Young, P. R., Fairlie, D. P., Juliano, L. (2007): Substrate specificity of recombinant dengue 2 virus NS2B-NS3 protease: influence of natural and unnatural basic amino acids on hydrolysis of synthetic fluorescent substrates. Archives of Biochemistry and Biophysics, 457, 187-196.

[61] Chappell, K.J., Stoermer, M.J., Fairlie, D.P., Young, P.R. (2006). Insights to substrate binding and processing by West Nile Virus NS3 protease through combined modeling, protease mutagenesis, and kinetic studies. Journal of Biological Chemistry, 281, 38448–38458.

[62] Noble, C. G., & Shi, P.-Y. (2012). Structural biology of dengue virus enzymes: Towards rational design of therapeutics. Antiviral Research, 96(2), 115–126.

[63] Chappell, K., Stoermer, M., Fairlie, D., & Young, P. (2008). West Nile Virus NS2B/NS3 Protease As An Antiviral Target. Current Medicinal Chemistry, 15(27), 2771–2784.

[64] Li, Z., Zhang, J., & Li, H. (2017). Flavivirus NS2B/NS3 Protease: Structure, Function, and Inhibition. Viral Proteases and Their Inhibitors, 163–188.

[65] Niyomrattanakit, P., Winoyanuwattikun, P., Chanprapaph, S. (2004): Identification of residues in the dengue virus type 2 NS2B cofactor that are critical for NS3 protease activation. Journal of Virology, 78(24), 13708–13716.

[66] Nitsche, C., Holloway, S., Schirmeister, T., & Klein, C. D. (2014). Biochemistry and Medicinal Chemistry of the Dengue Virus Protease. Chemical Reviews, 114(22), 11348–11381.

[67] De la Cruz, L., Nguyen, T. H. D., Ozawa, K., Shin, J., Graham, B., Huber, T., & Otting, G. (2011). Binding of Low Molecular Weight Inhibitors Promotes Large Conformational Changes in the Dengue Virus NS2B-NS3 Protease: Fold Analysis by Pseudocontact Shifts. Journal of the American Chemical Society, 133(47), 19205–19215.

[68] Falgout, B., Pethel, M., Zhang, Y.M., Lai, C.J. (1991): Both nonstructural proteins NS2B and NS3 are required for the proteolytic processing of dengue virus nonstructural proteins. Journal of Virology, 65, 2467.

[69] Li, L., Basavannacharya, C., Chan, K. W. K., Shang, L., Vasudevan, S. G., & Yin, Z. (2015). Structure-guided Discovery of a Novel Non-peptide Inhibitor of Dengue Virus NS2B-NS3 Protease. Chemical Biology & Drug Design, 86(3), 255–264.

[70] Llinàs-Brunet, M., Bailey, M., Fazal, G., Ghiro, E., Gorys, V., Goulet, S., Halmos, T., Maurice, R., Poirier, M., Poupart, MA., Thibeault, D., Lamarre, D. (2000). Highly potent and selective peptide-based inhibitors of the hepatitis C virus serine protease: towards smaller inhibitors. Bioorganic & Medicinal Chemistry Letters, 10(20), 2267–2270.

[71] Johnston, P. A., Phillips, J., Shun, T. Y., Shinde, S., Lazo, J. S., Huryn, D. M., Myers, M.C., Ratnikov, B. I., Smith, J. W., Su, Y., Dahl, R., Cosford, N. D., Shiryaev, S. A., Strongin, A. Y. (2007). HTS Identifies Novel and Specific Uncompetitive Inhibitors of the Two-Component NS2B-NS3 Proteinase of West Nile Virus. ASSAY and Drug Development Technologies, 5(6), 737–750.

[72] Rancourt, J., Cameron, D. R., Gorys, V., Lamarre, D., Poirier, M., Thibeault, D., & Llinàs-Brunet, M. (2004). Peptide-Based Inhibitors of the Hepatitis C Virus NS3 Protease: Structure−Activity Relationship at the C-Terminal Position. Journal of Medicinal Chemistry, 47(1), 2511–2522.

[73] De la Cruz, L., Nguyen, T. H. D., Ozawa, K., Shin, J., Graham, B., Huber, T., & Otting, G. (2011). Binding of Low Molecular Weight Inhibitors Promotes Large Conformational Changes in the Dengue Virus NS2B-NS3 Protease: Fold Analysis by Pseudocontact Shifts. Journal of the American Chemical Society, 133(47), 19205–19215.

[74] De la Cruz, L., Nguyen, T. H. D., Ozawa, K., Shin, J., Graham, B., Huber, T., & Otting, G. (2011). Binding of Low Molecular Weight Inhibitors Promotes Large Conformational Changes in the Dengue Virus NS2B-NS3 Protease: Fold Analysis by Pseudocontact Shifts. Journal of the American Chemical Society, 133(47), 19205–19215.

[75] Kang, C., Keller, T. H., & Luo, D. (2017). Zika Virus Protease: An Antiviral Drug Target. Trends in Microbiology, 25(10), 797–808.

[76] Nall, T. A., Chappell, K. J., Stoermer, M. J., Fang, N.-X., Tyndall, J. D. A., Young, P. R., & Fairlie, D. P. (2004). Enzymatic Characterization and Homology Model of a Catalytically Active Recombinant West Nile Virus NS3 Protease. Journal of Biological Chemistry, 279(47), 48535–48542.

[77] Chambers, T. J., Droll, A. A., Tang, Y., Liang, Z., Ganesh, V. K., Murthy, K. H., Nickells, M. (2005): Yellow fever virus NS2B-NS3 protease: characterization of charged-to-alanine mutant and revertant viruses and analysis of polyprotein-cleavage activities. Journal of General Virology, 86(5), 1403–1413.

[78] Keller T H, Chen Y L, Knox J E, Lim S P, Ma N L, Patel S J, Sampath A, Wang Q Y, Yin Z, Vasudevan S G. 2006. Finding new medicines for flaviviral targets. Novartis Found Symp, 277: 102-114; discussion 114-109, 251-103.

[79] Leung, D., Schroder, K., White, H., Fang, N.-X., Stoermer, M. J., Abbenante, G., Fairlie, D. P. (2001). Activity of Recombinant Dengue 2 Virus NS3 Protease in the Presence of a Truncated NS2B Co-factor, Small Peptide Substrates, and Inhibitors. Journal of Biological Chemistry, 276(49), 45762–45771.

[80] Yamaguchi, H., & Miyazaki, M. (2014). Refolding Techniques for Recovering Biologically Active Recombinant Proteins from Inclusion Bodies. Biomolecules, 4(1), 235–251.

[81] Zhang, Z., Li, Y., Loh, Y. R., Phoo, W. W., Hung, A. W., Kang, C., & Luo, D. (2016). Crystal structure of unlinked NS2B-NS3 protease from Zika virus. Science, 354(6319), 1597–1600.

[82] Bessaud, M., Pastorino, B. A. M., Peyrefitte, C. N., Rolland, D., Grandadam, M., & Tolou, H. J. (2006). Functional characterization of the NS2B/NS3 protease complex from seven viruses belonging to different groups inside the genus Flavivirus. Virus Research, 120(1-2), 79–90.

[83] Kim, Y. M., Gayen, S., Kang, C., Joy, J., Huang, Q., Chen, A. S., Wee, L. K., Ang, J. Y., Lim, H. A., Hung, A W., Li, R., Noble, C. G., Lee, L. T., Yip, A., Wang, Q. Y., Hill, J., Shi, P.Y., Keller, T. H. (2013). NMR Analysis of a Novel Enzymatically Active Unlinked Dengue NS2B-NS3 Protease Complex. Journal of Biological Chemistry, 288(18), 12891–12900.

[84] Shannon, A. E., Chappell, K. J., Stoermer, M. J., Chow, S. Y., Kok, W. M., Fairlie, D. P., & Young, P. R. (2016). Simultaneous uncoupled expression and purification of the Dengue virus NS3 protease and NS2B co-factor domain. Protein Expression and Purification, 119, 124–129.

[85] Tyndall, J. D. A., & Fairlie, D. P. (1999). Conformational homogeneity in molecular recognition by proteolytic enzymes. Journal of Molecular Recognition, 12(6), 363–370.

[86] Mueller, N. H., Yon, C., Ganesh, V. K., & Padmanabhan, R. (2007). Characterization of the West Nile virus protease substrate specificity and inhibitors. The International Journal of Biochemistry & Cell Biology, 39(3), 606–614.

References - Figure

[1] Sykes, J. E. (2016): Vector-borne and Other Viral Encephalitides. In: Veterian Key: Fastest Veterinary Medicine Insight Engine [online]. WordPress theme by UFO themes, [cit. 2021-02-11]. Available from: https://veteriankey.com/vector-borne-and-other-viral-encephalitides/.

[2] European Centre for Disease Prevention and Control. Introduction to the Annual Epidemiological Report. In: Annual epidemiological report for 2017 [Internet]. Stockholm: ECDC; 2017 [cited 24 July 2019]. Available from: http://ecdc.europa.eu/annual-epidemiological-reports/method.

[3] Pulkkinen, L. I. A,, Butcher, S. J., Anastasina, M. (2018). Tick-Borne Encephalitis Virus: A Structural View. Viruses, 10(7), 350.

[4] Shi, P.-Y. (2014). Unraveling a Flavivirus Enigma. Science, 343(6173), 849–850.

[5] Lindenbach, B.D., Murray, C.L., Thiel, H. J., Rice, C.M. (2007): Flaviviridae: The Viruses and Their Replication. Fields Virology, 5, 1101-1133.

[6] Li, K., Phoo, W. W., & Luo, D. (2014). Functional interplay among the flavivirus NS3 protease, helicase, and cofactors. Virologica Sinica, 29(2), 74–85.

[7] Noble, C. G., Chen, Y.-L., Dong, H., Gu, F., Lim, S. P., Schul, W., Wang, Q.-Y., Shi, P.-Y. (2010). Strategies for development of dengue virus inhibitors. Antiviral Research, 85(3), 450–462.

[8] Su, X.-C., Ozawa, K., Qi, R., Vasudevan, S. G., Lim, S. P., & Otting, G. (2009). NMR Analysis of the Dynamic Exchange of the NS2B Cofactor between Open and Closed Conformations of the West Nile Virus NS2B-NS3 Protease. PLoS Neglected Tropical Diseases, 3(12), e561.

[9] Li, Z., Zhang, J., & Li, H. (2017). Flavivirus NS2B/NS3 Protease: Structure, Function, and Inhibition. Viral Proteases and Their Inhibitors, 163–188.

[10] Luo, D., Vasudevan, S. G., & Lescar, J. (2015). The flavivirus NS2B–NS3 protease–helicase as a target for antiviral drug development. Antiviral Research, 118, 148–158.

8 Supplements

8.1 Cloning and expression vector

Expression plasmid pETDuet-1 (Novagen) was selected due to its two MSC, which allows for simultaneous production of two proteins in *E. coli*.

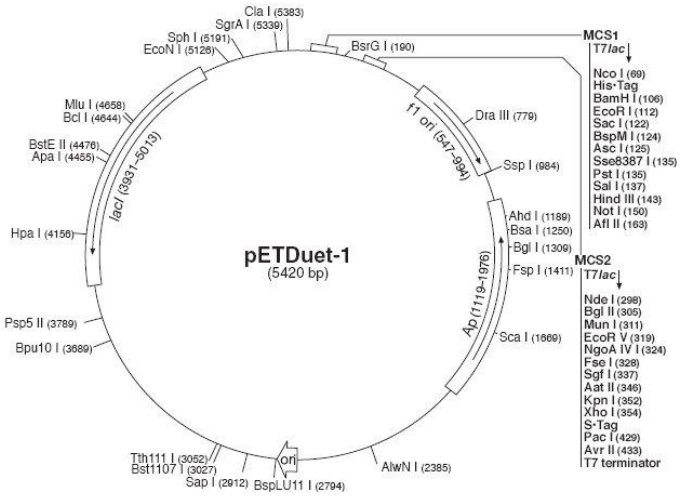

pETDuet-1 sequence landmarks	
T7 promoter-1	5404–5420
T7 transcription start-1	1
His•Tag® coding sequence	83–100
Multiple cloning sites-1 (*Nco* I–*Afl* II)	69–168
T7 promoter-2	214–230
T7 transcription start-2	231
Multiple cloning sites-2 (*Nde* I–*Avr* II)	297–438
S•Tag™ coding sequence	366–410
T7 terminator	462–509
lacI coding sequence	3931–5013
pBR322 origin	2737
bla (Ap) coding sequence	1119–1976
f1 origin	547–994

Figure 32: **The map of pETDuet-1**. NS2Bcof sequence was cloned into MCS1 and NS3pro, NS3proH was inserted into MCS2.

8.2 Competent bacterial cells

Three types of competent bacterial cells (Table 9) were used to conduct this experiment. Bacterial cells BL21 (DE3), NEB® 5-alpha were supplied by New England BioLabs,® Inc., and BL21 CodonPlus® by Agilent Technologies, Inc.

Table 9: **Competent bacterial cells**

Bacterial cell	**genotype**	**sensitivity**
BL21 (DE3) Competent *E.coli*	*fhuA2 [lon] ompT gal (λ DE3) [dcm] ΔhsdS λ DE3 = λ sBamHIo ΔEcoRI-B int::(lacI::PlacUV5::T7 gene1) i21 Δnin5*	**Amp,** Cam, Kan, Nit, Spec, Strep, Tet
NEB® 5-alpha Competent *E. coli* (High Efficiency)	*fhuA2 Δ(argF-lacZ)U169 phoA glnV44 Φ80 Δ(lacZ)M15 gyrA96 recA1 relA1 endA1 thi-1 hsdR17*	**Amp**, Cam, Kan, Nit, Strep, Spec, Tet
BL21 CodonPlus® competent Cells	*E. coli B F⁻ ompT hsdS(r_B^- m_B^-) dcm+ Tet^r gal λ (DE3) endA Hte metA::Tn5(Kan^r) [argU ileY leuW Cam^r]*	**Amp,** Cam, **Cam,** Kan, Nit, Strep, Tet

Note: (1) Antibiotic, that were used for selection, are highlighted in bold and underlined.

8.3 NS3, NS2B cofactor

8.3.1 DNA sequence NS2B cofactor Information on protein

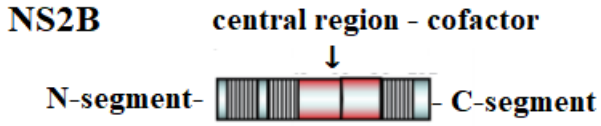

Figure 33: **Schematic representation of the flaviviral NS2B protein**. The central region is coloured in red. Adapted from [6].

AGAAAGATGCAGCTGGTTGCCGAATGGAGTGGCTGTGTGGAATGGCATCCGGA
ACTAGTGAATGAGGGTGGAGAGGTTAGCCTGCGGGTCCGTCAGGACGCGATG
GGAAACTTTCACTTGACTGAGCTCGAGAAAGAAGAGAGAATG

8.3.1.1 NS2Bcof protein sequence

RKMQLVAEWSGCVEWHPELVNEGGEVSLRVRQDAMGNFHLTELEKEERM

Number of amino acids: 49

Molecular weight: 5755.52 kDa

Theoretical pI: 4.98

Extinction coefficient: 11000 M^{-1} cm^{-1}

8.3.1.2 NS2Bcof with N- terminal His-tag (in pETDuet-1)

MGSSHHHHHHSQGSRKMQLVAEWSGCVEWHPELVNEGGEVSLRVRQDAMGNF

HLTELEKEERM

Number of amino acids: 63

Molecular weight: 7300.10

Theoretical pI: 6.01

Ext. coefficient: 11000 $M^{-1}cm^{-1}$

8.3.2 DNA sequence NS3 protease

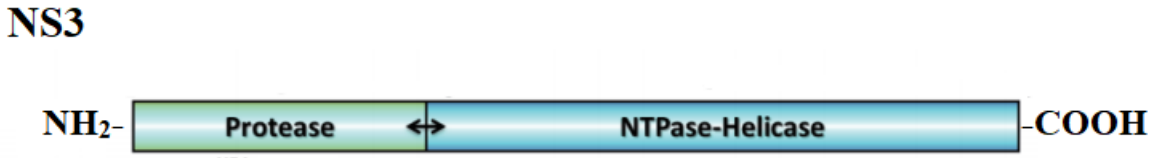

Figure 34: **Schematic representation of the flaviviral NS3 protein.** Protease is in green colour, NS3hel is in blue. Adapted from [6].

8.3.2.1 DNA sequence encoding TBEV NS3pro

5′TCTGACCTGGTTTTCTCTGGACAGGGGGGTCGAGAGCGTGGTGACAGACCTT
TCGAGGTTAAGGACGGTGTCTACAGGATTTTCAGCCCCGGCTTGTTCTGGGGTC
AGAACCAGGTGGGAGTTGGCTACGGTTCCAAAGGTGTCTTGCACACGATGTGG
CATGTGACGAGAGGAGCGGCGCTGTCTATTGATGATGCTGTGGCCGGTCCCTA
CTGGGCTGATGTGAGGGAGGATGTTGTGTGCTACGGAGGAGCCTGGAGTCTGG
AGGAAAAATGGAAAGGTGAAACAGTACAGGTTCATGCCTTCCCACCAGGGAA
GGCCCATGAGGTGCATCAGTGCCAGCCTGGGGAGTTGATCCTTGACACCGGAA
GGAAGCTTGGGGCAATACCAATTGATTTGGTAAAAGGAACATCAGGCAGCCCC
ATTCTTAACGCCCAGGGAGTGGTCGTGGGGCTATACGGAAATGGCCTAAAGAC
CAATGAGACCTACGTCAGCAGCATTGCTCAAGGGGAAGCGGAGAAGAGTCGA
CCCAACCTCCCACAGGCTGTTGTGGGCACGGGCTGGACATCA – 3′

8.3.2.2 Protein sequence NS3pro (in pETDuet-1)

SDLVFSGQGGRERGDRPFEVKDGVYRIFSPGLFWGQNQVGVGYGSKGVLHTMW

HVTRGAALSIDDAVAGPYWADVREDVVCYGGAWSLEEKWKGETVQVHAFPPGK

AHEVHQCQPGELILDTGRKLGAIPIDLVKGTSGSPILNAQGVVVGLYGNGLKTNET

YVSSIAQGEAEKSRPNLPQAVVGTGWTS

Number of amino acids: 190

Molecular weight: 20305.79 kDa

Theoretical pI: 5.94

Extinction coefficient: 41940 $M^{-1}cm^{-1}$

8.3.2.3 Protein sequence NS3proH (in pETDuet-1)

MSDLVFSGQGGRERGDRPFEVKDGVYRIFSPGLFWGQNQVGVGYGSKGVLHTM
WHVTRGAALSIDDAVAGPYWADVREDVVCYGGAWSLEEKWKGETVQVHAFPP
GKAHEVHQCQPGELILDTGRKLGAIPIDLVKGTSG SPILNAQGVVVGLYGNGLKT
NETYVSSIAQ GEAEKSRPNL
PQAVVGTGWT SHHHHHH

Number of amino acids: 197

Molecular weight: 21259.83

Theoretical pI: 6.40

Ext. coefficient: 42065 $M^{-1}cm^{-1}$

8.3.3 Information on recombinant NS2Bcof+NS3pro

Number of amino acids: 239

Molecular weight: 26

Number of a 043.29 kDa

Theoretical pI: 5.53

Extinction coefficient: 52940 M^{-1} cm^{-1}

8.3.4 Information on recombinant NS2Bcof-NS3proH

MGSSHHHHHHSQGSRKMQLVAEWSGCVEWHPELVNEGGEVSLRVRQDAMGNF
HLTELEKEERMMSDLVFSGQGGRERGDRPFEVKDGVYRIFSPGLFWGQNQVGVG
YGSKGVLHTMWHVTRGAALSIDDAVAGPYWADVREDVVCYGGAWSLEEKWKG
ETVQVHAFPPGKAHEVHQCQPGELILDTGRKLGAIPIDLVKGTSGSPILNAQGVVV
GLYGNG LKTNETYVSS IAQGEAEKSRPNLPQAVVGT GWTSHHHHHH

Number of amino acids: 260

Molecular weight: 28541.92

Theoretical pI: 6.24

Ext. coefficient: 53065 $M^{-1}cm^{-1}$

8.4 Protease assay

Protease assay with an inhibitor was done. Aprotinin was used as an inhibitor (delivered by Sigma®). Protease assay set up follow part 4.8.

Table 10: **Protease assay set up with an inhibitor**

	Final concentration in 25 µL	**Final concentration in 50 µL**	**Final concentration in 100 µL**
Protease	16 µM	8 µM	4 µM
ZRR-AMC	400 µM	200 µM	100 µM
Inhibitor	160 µM	80 µM	40 µM

Note: Total volume composition per well was 50 µL of protease, 25 µL of substrate and 25 µL of inhibitor

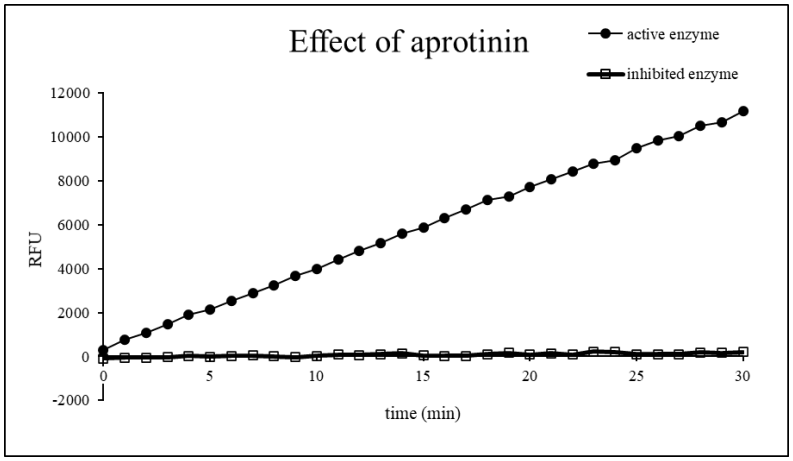

Figure 35: **Enzymatic characterazion of NS2B-NS3pro. Efects of inhibitor aprotinin.**